Appendix 9
Risk Methodology

Introduction

This Appendix describes the risk analysis philosophy and methodology used to evaluate the performance of the New Orleans hurricane protection system. Probabilistic risk analysis as described by Ayyub (2003), Kumamoto and Henley (1996), and Modarres et al. (1999) was used to develop the basic risk analysis methodology of the hurricane protection system. The basic elements of the risk analysis methodology are illustrated in the flow chart presented in Figure 9-1. The analysis was developed as a series of modules which interface to provide a risk model for the New Orleans HPS. An Excel spreadsheet program, Flood Risk Analysis for Tropical Storm Environments (FoRTE), was developed to implement the many water volume calculations and exceedance values required to determine the risk of inundation for the suite of hurricanes investigated. The spreadsheet (FoRTE) is described in Appendix 17. The results of the many FoRTE program runs were post processed and modified to include wave runup, interflow between sub-basins for the aggregated storm water volumes, and pumping, and to adjust the program outputs based on historic experience. The results of the analyses are described in Appendix 13.

In the engineering community, *risk* is generally defined as the potential that a component or system will incur losses from exposure to a hazard or as a result of an uncertain event. Risk is quantified as the rate (measured in events per unit time) that lives, economic, environmental, and social and cultural losses will occur due to the non-performance of an engineered system or component. The non-performance of the system or component can be quantified as the probability that specific loads (or demands) exceed respective strengths (or capacities) causing the system to fail, and losses if that failure occurs. Risk can be viewed to be a multi-dimensional quantity that includes event-occurrence rate (or probability), event-occurrence consequences, consequence significance, and the population at risk; however, it is commonly measured as a pair of the rate (or probability) of occurrence of an event, and the outcomes or consequences associated with the event's occurrence that account for system weakness, i.e., vulnerabilities. Another common representation of risk is in the form of an exceedance rate (or probability) function of consequences. In a simplified form, risk is commonly expressed as:

$$Risk = Event\ rate\ (or\ probability) \times Vulnerability \times Consequences\ of\ failure$$

This equation not only defines risk but also offers strategies to control or manage risk, i.e., by making the system more reliable or by reducing the potential losses resulting from a failure. The vulnerability, or probability of failure, part of the equation can be influenced by engineers by strengthening of existing structures, increasing reliability or by adding additional protection. However, the consequence part is highly dependent upon the actions and decisions made by residents, government and local officials, including first-response and evacuation plans and practices. In densely populated areas, simply increasing system reliability may not reduce risks to acceptable levels and increasing consequences through continued flood plain development can offset any risk reductions or cause an increase in risk.

A reliability analyses is used to model the performance of individual elements and features (such as, floodwalls, levees, pumps, levee closures, etc.) located throughout the hurricane protection system to the overall performance of the integrated HPS. The reliability of the various elements and features considers the varying material properties of the structures and of foundation conditions that exist throughout the HPS. The impact of this performance on public safety and, social and economic welfare is incorporated into the risk analysis.

Implementation of risk analysis to the HPS of New Orleans and S.E. Louisiana was challenging because it is a complex system of levees, floodwalls and pumping stations, constructed over many years by different entities that serve a large geographical region. In addition, existing capability to accurately predict and model hurricanes in regions as complex as the Mississippi delta was limited. Nonetheless, mathematical modeling of hurricanes and risk analysis methodologies have improved greatly in recent years to make them important, viable tools for supporting investment decisions as the HPS is restored and improved. In developing the risk analysis strategy, the following requirements were identified as key guiding principles:

- **Analytic.** The methodology must provide a systematic framework for assessing risk by decomposing risk into its basic elements.
- **Transparent.** All assumptions and analytical steps are clearly defined.
- **Defensible.** Values for each parameter are supported by all available data, including knowledge from previous studies and expert opinion.
- **Quantitative.** Risk is expressed in meaningful and consistent units (e.g., dollars and fatalities) so as to provide a basis for performing tradeoffs and benefit-cost analysis.
- **Probabilistic.** The mathematics of probability theory is used for expressing uncertainty in all model parameters and assessing the likelihood of alternative scenarios.
- **Consistent.** It is consistent with established and accepted practices of probabilistic risk assessment (PRA) used in many other fields.

The quantification of risk also required that the analysis consider uncertainty in both the input values and the modeling capabilities. For example, detailed knowledge of the engineering parameters that influence the performance of the HPS and of the hurricane characteristics of storms expected to impact New Orleans is limited. This includes properties of foundation soils underlying the extensive levee and floodwall system, and the frequency with which hurricanes will occur in the future. As other examples, Dixon, et al. (2006) provides an overview of subsidence and flooding in New Orleans; Dokka (2006) describes the tectonic subsidence in coastal Louisiana; and Muir-Wood and Bateman (2005) describe uncertainties and constraints on

breaching and their implications for flood loss estimation. Hurricane models can predict winds, waves and surges only with limited accuracy, and the reliability models used to predict levee performance when subjected to hurricane forces are similarly limited. Hence, the risk profiles of hurricane-induced flooding cannot be established with certainty. Risk analysis, therefore, must include not just a best estimate of risk, but also an estimate of the uncertainty in that best estimate. By identifying the sources of uncertainty in the analysis, measures such as gathering additional data can be taken to reduce the uncertainty and improve the risk estimates.

Several key considerations and limitations of the IPET risk study which should be noted are:

- Defining the physical features of the system required an accurate inventory of all components that provide protection against storm surge and waves. This included cross sections, strength parameters of components, transitions between elements, crest elevations and foundation conditions along reaches. The characterization of the physical features of the protection system was, however, limited by the availability of up-to-date information, the resources to conduct detailed field surveys, and the ability to process the large amount of information that was changing during the course of the study.

- The hurricane modeling and reliability analyses required an accurate depiction of the elevations of the tops of levees and walls that make up the HPS. This was complicated by the different datum used in the area over many years, the lack of up-to-date pre-Katrina survey data and the damage caused by Katrina. The risk team utilized the work by other IPET teams to define the datum to be used. The datum used for all elevations cited in the risk study was NAVD88 2004.65. The risk team used data provided by the New Orleans District, Task Force Guardian and others to establish the pre- and post-Katrina crest elevations.

- The pumping system is an important element of the HPS that controls flooding during and after rain and tropical storms, but was not designed to handle overtopping and breaching during hurricane events. This is also complicated by the human factors that affect the operation of the pumping system. For these reasons, several levels of pumping performance were investigated to provide a range of potential performance levels.

- The consequences associated with pre- and post-Katrina flooding are different due to changes in population and economic activity.

- The effectiveness of the protection system depends on human factors as well as engineered systems (e.g., timely road and railroad closures, gate operations, and functioning of pumping stations). Lessons learned from Katrina and other natural disasters were used in modeling the closures.

- Wave runup, interflow between sub-basins for aggregated storm water volumes, and pumping was considered outside of the FoRTE program using a simplified analysis. Adjustments to the FoRTE outputs were based on historic data.

Key Factors Influencing Risk

The development of a risk analysis model was facilitated by the preparation of an influence diagram. The process of creating an influence diagram helped establish a basic understanding of the elements of the hurricane protection system and their relationship to the overall system performance during a hurricane event and defined input required for the analysis of consequences and risks.

Figure 9-2 shows the influence diagram for the hurricane protection system and the analysis of consequences. There are four parts to the influence diagram:

- Value nodes (rounded-corner box)
- Chance nodes (circular areas)
- Decision nodes (square-corner boxes)
- Factors and dependencies in the form of arrows.

The influence diagram was used to develop an event (or probability) tree for the hurricane protection system. Figure 9-3 shows an initial probability tree derived from the influence diagram in Figure 9-2. The top events across the tree identify the random events whose state following the occurrence of the hurricane could contribute to flooding in a protected area. The tree begins with the initiating event which is a hurricane that generates a storm surge, winds and rainfall in the region.

Analysis Boundaries

An important initial step in the analysis is to clearly define the bounds of the study and the physical descriptions of the various components of a HPS. These bounds included defining the geographic bounds of the study region, the elements of the hurricane protection system, the resolution of information and analyses to be performed, and analysis constraints or assumptions associated with the risk and reliability analyses.

Study Region and Hurricane Protection System

Figure 9-4 identifies the region of southeast Louisiana considered and the major parishes of the area protected by the hurricane protection system. The HPS study area is limited to the six parishes that make up the metropolitan New Orleans area.

Physical Description of the HPS

The HPS is comprised of a variety of sub-systems, structures, and components, which include earthen levees, floodwalls, pumping stations, drainage canals, road and railway closures, and power supply systems. The system is a combination of low lying tracts surrounded by flood

barriers that form drainage basins, which are independently maintained and operated by local parishes and levee boards. Detailed physical descriptions for each basin based on current conditions are provided by Appendices 2 through 7. Data collected during site inspections by the risk team were used to define characteristics of the basins and their interdependence for use in the risk model. This was a critical and time consuming step in the development of the risk model that has yielded a comprehensive description of the HPS. These descriptions were developed by examining available information gathered by IPET including:

- Design memorandums and supporting documents,
- Pre- and post-Katrina construction documents,
- Inspection reports,
- Katrina damage reports, and
- Detailed field surveys conducted by the Risk Team to verify the location and configurations of the HPS.
- Comprehensive studies conducted by other IPET teams
- Information collected by Task Force Guardian during repair of the HPS.

The information gathered was incorporated into detailed geographic information system (GIS) based maps of each basin that included: locations of all features (walls, levees, pumping stations, and closure gates), geotechnical information (boring logs, geologic profiles), aerial photographs, photos of each feature and elevations of the tops of levees and walls.

Analysis Assumptions and Constraints

As part of the process of developing the risk analysis model, it was necessary to identify key assumptions and analysis constraints. Constraints refer to events or situations that were not modeled or considered explicitly in the analysis. The analysis limitations or constraints of the risk model development are summarized by the following:

- Only modeling procedures that existed prior to Katrina were used.

- Geographic area was limited to elements of the hurricane protection system in the following basins:
    - St. Charles
    - Jefferson (East and West Bank)
    - Orleans (East and West Bank)
    - New Orleans East
    - St. Bernard
    - Plaquemines

- The risk model does not produce temporal profiles, but rather spatial profiles accumulated over the durations of respective storms.

- The risk model includes assumptions based on the information collected to select the parameters used in various major aspects of the hurricane protection system

characterization, hurricane simulation, reliability analysis, inundation analysis, and consequence analysis.

- Hazards, and thus consequences, not considered in the risk analysis are: wind damage to buildings, fire, civil unrest, indirect economic consequences, effect of a release of hazardous materials, and environmental consequences.

- The performance of the evacuation plan New Orleans was not modeled in the risk analysis.

Hurricane Protection System

The hurricane protection system (HPS) for the New Orleans metropolitan area shown in Figure 9- 4 is sub-divided into basins that follow parish boundaries and sub-basins that define the interior drainage characteristics of the basins. Basins and sub-basins are divided into sections, or reaches, that have similar cross-sections, material strength parameters and foundation conditions. Features such as: pumping stations, road and railway closures, drainage structures, etc. within a reach are defined as points within the reach that have the potential for allowing water inflow in the event of their failure. The HPS has been discretized for the reliability and risk analysis tasks as schematically shown in Figure 9- 5 which shows an example of how the HPS was discretized to define the system in the risk model. A complete definition of the system is provided in the appendices. The system consists of basins, sub-basins, reaches, features, and transitions. The definitions of these components of the HPS are based on the following considerations:

- Local jurisdiction,

- Floodwall type and cross section,

- Levee type and cross section,

- Engineering parameters defining structural performance,

- Soil strength parameters,

- Foundations parameters,

Reaches of each basin are uniquely identified using sequential numbers as illustrated in the Figure 9-5. The figure also shows the approximate locations of pumping stations for the purpose of illustration.

Definition of Basins, Sub-basins, Reaches and Features

The hurricane protection system is divided into basins, sub-basins, reaches, features and transitions. Table 9-1 illustrates the information structure needed for this definition for selected reaches. The definition includes the following basins with their respective numeric identification:

1. Orleans West Bank (OW)
2. New Orleans East (NOE)
3. Orleans (OM)
4. St. Bernard (SB)
5. Jefferson East (JE)
6. Jefferson West (JW)
7. Plaquemines Area (PL)
8. St. Charles (SC)

Reach Descriptions

The HPS perimeter is discretized into reaches that define sections that have similar physical and engineering characteristics. Initially the reaches were defined using the beginning and ending stations shown in the design memoranda (DM). The stations were then adjusted based on examinations of the subsurface material information to form reaches that were expected to have similar performance (reliability). For each reach, the following information, as shown in Table 9-1, is required:

- Reach numeric identification that can be associated with a unique station in hurricane simulation
- Reach length (ft)
- The reach crest elevation (ft)
- Reach type, either a levee (L) or a floodwall (W)
- Reach weir coefficient needed to compute overtopping water volume of either 2.6 for a levee or 3.0 for a floodwall (in units of ft and sec)
- Basin reference that defines the location of the reach in reference to the overall HPS
- Sub-basin reference that defines where water from overtopping or breaching of the reach will collect.

Table 9-1. Definition of Reaches						
Reach No.	**Length (ft)**	**Elevation (ft)**	**Design Water Elevation (ft)**	**Reach Type**	**Reach Weir Coefficient**	**Subbasin Reference**
1	5,000	14.00	8.00	Levee	2.6	Basin1-1
2	10,000	15.00	9.00	Floodwall	3.0	Basin1-2
3	22,500	16.00	11.00	Levee	2.6	Basin1-3
4	6,000	14.00	10.00	Floodwall	3.0	Basin1-4
5	9,000	18.00	13.00	Levee	2.6	Basin1-5
6	7,000	14.00	8.00	Levee	2.6	Basin2-1
7	11,000	15.00	9.00	Floodwall	3.0	Basin2-2
8	7,500	16.00	11.00	Levee	2.6	Basin2-3
9	500	11.00	8.00	Transition	3.0	Basin1-2
10	400	12.00	8.00	Transition	2.6	Basin2-2

Feature Descriptions

Table 9- 2 illustrates the definitions of features within each reach for selected reaches. For each feature, the following information is required:

- Feature number for unique identification
- Type of features of drainage structure (D), or closures (i.e., gate G), or transition structure (T)
- Reach reference where the feature is located
- A reference value for correlated gates for assigning the same probability of closure
- Width of opening (ft) for water inflow through open gates
- Bottom elevation (ft) of gates
- Probability of gate not closed during a hurricane

Table 9-2. Definition of Features with Respective Reaches					
Feature No.	**Reach No.**	**Correlated Features**	**Length (ft)**	**Bottom Elevation (ft)**	**Not-closed Probability**
1	1	1	500	5.00	0.10
2	1	1	500	5.00	0.15
3	2	3	400	6.00	0.10
4	2	3	400	7.00	0.20
5	2	3	400	5.00	0.10
6	3	3	600	5.00	0.15
7	4	7	600	7.00	0.20
8	4	8	600	6.00	0.10
9	5	9	500	6.00	0.10
10	5	9	500	5.00	0.01

Sources of Information

The Risk Team collected data from design documents, construction drawings and studies conducted by other IPET teams to develop detailed descriptions of the basins. Maps were assembled from aerial photos and information was overlayed in GIS files that included: lat/long data, geotechnical profiles and boring logs, crest elevations, stationing used to define reaches and the locations of critical features such as closure gates and pump stations. The information on these maps was confirmed by field surveys of the entire system by members of the Risk Team who traveled every mile of the system. Photos, GPS coordinates and notes were taken during these surveys to document each feature and reach used in the risk model. In addition to the maps, data was compiled for use in the reliability analyses and the risk model. This process has resulted in a comprehensive description of the HPS. The basin descriptions are provided in Appendices 2 thru 7.

Elevations of Crests

The elevations of the tops of walls and levees, adjusted to the current datum, of the entire New Orleans area HPS were developed for use in the suite of hurricane simulations and the risk assessment model calculations of water volumes from overtopping and breaching. Various sources for elevations of segments of the HPS existed; some adjusted to current datum, but most were not. The 1 ft^2 and 15 ft^2 lidar data on the IPET repository have been adjusted to current datum and gave about 99% coverage of the HPS system. The adjusted lidar data gave good values for portions of the HPS that had levees that were clear of vegetation. In addition, there were numerous field surveys that were available for short portions of the walls, some of which been adjusted to the latest datum.

Using the 1 ft^2 lidar where it was available, cross section profiles were created for lengths of approximately 200 to 500 ft along the entire HPS. Where the 1 ft lidar was not available, the 15 ft^2 lidar was used. For the levees, these elevations were compared to the current expected values obtained from various MVN records, Taskforce Guardian, and any available field survey information for verification. The location of walls, drainage structures, closures, and gaps were

known from the field survey of the entire HPS that was documented with photos and notes. Some walls had adjusted survey information available, but for most walls it was necessary to go back to the lidar data and examine the areas by drawing numerous profiles, searching for lidar data patterns of "good hits" on wall tops and determining the elevations of the surrounding soil. Then, using the photos and notes obtained from the site visits, estimates of the wall elevations were made. This same process was used for transition regions. A final comparison to the elevations used in the grid developed by the Storm Team for use in the computer program ADCIRC was made for consistency.

Performance of HPS Structures

The performance of the structures providing hurricane protection against potential water elevations due to surge and waves was quantified using structural and geotechnical reliability models integrated within a larger system description of each drainage basin. The reliability models for the HPS components were developed based on design and construction information, and on the results of the IPET Performance Team and the Pump Stations Team studies. Reliability models were developed and evaluated to determine dominant, or most likely, failure modes for each reach defined in a drainage basin. Failure modes, performance functions, basic random variables, and computational procedures used to model failure probability are provided in Appendix 10, Reliability Methodology.

The reliability models included uncertainties in structural material properties, geotechnical engineering properties, subsurface soil profile conditions, and engineering performance models of levees, floodwalls, and transition points. Uncertainties due to spatial and temporal variation and due to limited knowledge are tracked separately in the analysis. The reliability models provided a best estimate of the frequency of failure under given loads, along with a measure of the uncertainty in that frequency.

Engineering performance models and calculations were adapted from the Geotechnical Design Manuals (GDM) and engineering parameter and model uncertainties were propagated through those calculations to obtain approximate fragility curves as a function of water height for components of the HPS. These results were calibrated against the analyses of the Performance Team, which applied more sophisticated analysis techniques to similar structural and geotechnical profiles in the vicinity of failures. Failure modes identified by the Performance Team were incorporated into the reliability analyses as those results became available.

Reliability assessments were performed for individual reaches of the HPS for given water elevations. The assessments resulted in fragility curves for each reach by dominant or most likely mode of failure. A fragility curve gives the probability of failure, conditional upon an event (water elevation in this study), at which a limiting failure state is exceeded. A sample fragility curve is shown in Figure 9-6 and the actual curves used in the risk analysis are shown in Appendix 10.

Hurricane Hazard Analysis

The hurricane hazard analysis method parameterizes hurricanes using their characteristics at landfall. The hazard analysis was conducted by an independent team that included representatives from USACE, FEMA, consulting firms and academia. Details of the analysis are presented in Appendix 8. The following parameters were considered:

- Central pressure deficit at landfall,
- Radius to maximum winds at landfall,
- Longitudinal landfall location relative to downtown New Orleans,
- Track of storm motion at landfall,
- Storm translation speed at landfall, and
- Holland's radial pressure profile parameter at landfall (Holland 1980).

Using parameter values based on historic events, the recurrence rate and the joint probability density function of the hurricane parameters were estimated for hurricane events in the New Orleans region of interest. The parameters used by the hurricane team to develop the storms they provided to the risk team are shown in Table 9-3. Note that frequencies of the storms highlighted in yellow in Table 9-3 were not provided; therefore, these hurricanes were not used in the risk analysis.

The selected hurricanes were used as input to the ADCIRC models which used several finite element grids for the various conditions of the HPS. The grids corresponded to the condition of the HPS before Katrina and after repairs and improvements had been completed following Katrina.

Since the possible combinations of winds, surges and waves would be computationally demanding if every combination was run through the ADCIRC models, the number of runs was reduced by using a response surface approach. In this approach a relatively small number of hurricanes were selected and used to calculate the corresponding surge and wave levels at the sites of interest. Then a response surface model was fitted to each response variable (surge or wave level at a specific site). Finally, a refined discretization of the parameter space was used with the response surface to represent the hurricane hazard. The outcomes of these computations were combined surge and effective wave setup elevations at particular locations of interest along the hurricane protection system, e.g., representative values at points along the reaches.

A hydrograph with time-varying surge plus wave setup elevations at each reach was produced, based on the ADCIRC analyses, and provided as input to the risk model. Example hydrographs for a single reach are show in Figure 9-7. Wave runup elevations were added using a simplified approach.

Risk Quantification

The quantification of risk associated with a hurricane protection system required establishing a performance measure for the HPS. The selected performance measure was the amount of water expected to enter protected areas during a particular hurricane. The water entered protected areas as a result of one or more of the following cases:

1. Non-breach events such as overtopping, water entering through closures (i.e., gates) that are left open, precipitation, and potential backflow from pumping stations

2. Breaching events caused by levee or flood wall failure that lead to water inflow into protected areas

3. Rainfall during hurricane events

The risk quantification framework has, therefore, the objective of estimating water volumes and elevations in basins according to these cases. The event tree presented in Figure 9-8 shows the quantities of interest in the net water levels (W) column resulting from open closures, overtopping, breaching, and operation of pumping stations in non-breach cases. The branches for the rainfall volume are shown separately for clarity, but were added to all the other branches during calculations. Figure 9-8 shows a total of 12 branches that were evaluated for each hurricane. These branches were numbered sequentially as shown in the event tree. The top events of the tree are defined in Table 9-3.

The results for each storm event were evaluated by aggregating the individual results for each basin. This provided an estimate of water inundation volumes in each basin along with the frequencies of occurrence. These were then converted to elevations using the stage-storage curves for each basin thereby yielding elevation – exceedance relationships. The evaluation of consequences relative to basin inundation levels were provided by the Consequence Team based upon the elevations selected for the 50, 100 and 500 year events.

Table 9- 3
Summary of the Event Tree Top Events

Top Event	Description
Hurricane initiating event	The hurricane initiating event maps the peak flood surge and wave effects with a hurricane rate λ. This event can be denoted, hi(x,y), and has a probability of occurrence, P(hi(x,y)) and a rate of occurrence of λP(hi(x,y)).
Closure structure and operations (C)	The closure event models whether the hurricane protection system closures, i.e., gates, have been sealed prior to the hurricane. This event depends on a number of factors, as illustrated in the influence diagram. The closure structures were grouped by basins in terms of probability of being closed in preparation for the arrival of a hurricane. This event can be used to account for variations in local practices and effectiveness relating to closures and their operations.
Precipitation inflow (Q)	The precipitation event models the rainfall that occurs during a hurricane event. The precipitation inflow per subbasin is treated as a random variable.
Drainage, pumping and power (P)	The drainage event treats pumping in aggregate with drainage effectiveness and power reliability, including backflow through pumps.
Overtopping (O)	This event models the failure of the HPS due to overtopping.
Breach (B)	The breach event models the failure of the HPS during the hurricane. This event includes all failures other than overtopping. This event is treated using conditional probabilities as provided in Figure 9-8.

Risk associated with the hurricane protection system was quantified through a regional hurricane rate (λ) and the probability $P(C > c)$ where a consequence measure C exceeds different levels c. The loss exceedance probability per event was evaluated as

$$P(C > c) = \sum_i \sum_j P(h_i) P(S_j \mid h_i) P(C > c \mid h_i, S_j) \quad (9\text{-}1)$$

An annual loss exceedance rate was estimated as follows

$$\lambda(C > c) = \sum_i \sum_j \lambda P(h_i) P(S_j \mid h_i) \times P(C > c \mid h_i, S_j) \quad \text{Eq. (9-2)}$$

where $P(h_i)$ is the probability of hurricane events of type i, $P(S_j|h_i)$ is the probability that the system is left in state j from the occurrence of h_i, and $P(C > c \mid h_i, S_j)$ is the probability that the consequence C exceeds level c under (h_i, S_j). Summation was over all hurricane types i and all system states j in a suitable discretization. Simulation studies of hurricanes for risk analysis required a set of hurricane cases h_i and their respective rates of occurrence λ_i.

Evaluation of the regional hurricane rate λ and the probability $P(h_i)$, the conditional probabilities $P(S_j \mid h_i)$, and the conditional probabilities $P(C > c \mid h_i, S_j)$ was obtained from the hurricane model, the HPS risk assessment model, and the consequence model, respectively.

Water Inflow Volume Models

The hydrographs and HPS system descriptions and fragilities were used to compute whether water entered a basin by levee overtopping or breach, and to determine the resulting water elevation (H_{ps}) within the basin. In the case of levee overtopping, H_{ps} within a basin was based on the water volume computed using the duration of overtopping. If a breach occurred and the invert of the breach was below the final elevation of an adjacent body of water, H_{ps} was set to the elevation of that body of water. If the breach invert was above the final elevation of an adjacent body of water, H_{ps} was based on a water volume computed using the duration that the surge elevation was above the breach invert. The topography, stage-storage curves, and the drainage and pumping models for a basin were used to construct such a relationship. The major basins were subdivided into sub-basins according to the drainage and pumping characteristics within the basin. These subdivisions are show in Figure 9-9.

Water Volumes from Other Features of the Protection System. The hurricane protection system includes features that could allow water volume to enter the protected areas during a hurricane. These features include:

1. Closure structures, i.e., gates, that were left open or failed to close

2. Local changes in elevations at transitions in the HPS, typically between levees and floodwalls

These features are identified within each reach and assigned to a subbasin. The water volume resulting from failure of closure structures for a given hurricane was computed using the closure structure failure probability, width of the closure structure, and the elevation at the bottom of the structure. The water volume associated with localized changes in transitions required the change in elevation and the lengths over which the elevation varied.

Table 9-4. Sample Reach Overtopping Volume Results

Hurricane Run No.	Hurricane Rate (events/ year)	Overtopping Volume (ft^3)					
		For Basin1-1		For Basin1-2		For Basin2-1	
		Mean	Standard Deviation	Mean	Standard Deviation	Mean	Standard Deviation
1	1.00E-01	0.00E+00	0.00E+00	0.00E+00	0.00E+00	8.28E+07	1.66E+07
2	5.00E-02	0.00E+00	0.00E+00	0.00E+00	0.00E+00	1.07E+08	3.31E+07
3	1.00E-02	6.57E+07	1.22E+07	8.28E+07	1.66E+07	8.28E+07	1.66E+07
4	1.00E-02	7.87E+07	2.11E+07	8.28E+07	1.66E+07	8.28E+07	1.66E+07
5	1.00E-02	0.00E+00	0.00E+00	0.00E+00	0.00E+00	9.67E+07	3.30E+07
6	1.50E-01	0.00E+00	0.00E+00	0.00E+00	0.00E+00	7.92E+07	1.89E+07
7	5.00E-03	1.24E+08	2.39E+07	1.90E+08	3.76E+07	1.90E+08	3.76E+07
8	9.00E-02	8.69E+07	2.99E+07	7.99E+07	1.99E+07	6.78E+06	1.79E+07
9	1.00E-02	0.00E+00	0.00E+00	0.00E+00	0.00E+00	1.03E+08	2.43E+07
10	5.00E-02	0.00E+00	0.00E+00	0.00E+00	0.00E+00	1.03E+08	3.21E+07

Pumping, Rainfall and Total Water Volume in a Subbasin. The total volume entering a sub-basin (as a random variable with mean and standard deviation) was calculated for each branch of the event tree by summing volumes of water due to overtopping, breaching, and closure structures, as well as the water volume from rainfall and wave runup minus the effect of pumping.

The pumping system in New Orleans was designed to remove rainfall from tropical storms up to about a 10-year event. The effect of pumping on sub-basin inflow water volumes was approximated by subtracting a portion of the 10-year rainfall (that considered degraded pump reliabilities and efficiencies) as a function of water level accumulated in a sub-basin. The water volume that could be pumped by a given pump station within a particular subbasin was estimated by taking the total individual pump station capacity and multiplying it by the duration of the intense portion of the rainfall for each storm. These volumes were then summed for all the stations within a sub-basin. This volume was considered to be the 100-percent pump station capacity and was subtracted from the rainfall of storm, up to the estimated 10-year rainfall volume. Volumes were also determined for 50-percent pump station capacity and no pump station capacity.

Water Interflow between Basins and Sub-basins. Within a basin, water entering a sub-basin may, under certain conditions, overflow into adjacent sub-basins. Thus, prior to calculating the final volume of water in the sub-basins for each of the 16 branches in the event tree of Figure 9-8, interflow among sub-basins was considered. This was done by modeling the elevations of the interfaces between sub-basins and determining the volume of water that would

pass between sub-basins for the amount of time the interface elevation was exceeded. Table 9-4 shows a tabulated structure for computing volumes associated with sub-basins.

Breaching Models

Three cases of breach failure were examined that corresponded to the breaching branches presented in the event tree of Figure 9- 8. The three cases are:

1. Breach given overtopping
2. Breach given no overtopping
3. Breach due to feature (closure gate, pump house, etc.) or transition failures

The first case of breach given overtopping is primarily driven by erosion, resulting from overtopping water flow. Fragility curves for these cases were developed as described in the Reliability Methodology (Appendix 10). Table 9-5 summarizes the breaching model used in the risk analysis.

Breach Parameters

The breaching scenarios require knowledge of the average breach length and depth and of the hydrograph at the breach location to determine basin inflows. The HPS condition after Katrina was reviewed to identify basic characteristics of the major breaches. The identified characteristics were used to develop general rules for estimating breach dimensions in the risk model. One critical characteristic for determining the volume of water flowing through a breach is the duration of time that the breach is open. During Katrina, the breaches could not be repaired in time to have an effect on the level of water achieved inside the basins. Therefore the time at which the breach occurred was assumed to have no effect on inflow volumes and water elevations.

Breach without Overtopping

IPET studies indicated that the London Ave. and 17th St. Canal breaches occurred during Katrina before the water level in the canals reached the top of the floodwall; the breaches appeared to have been the result of a foundation and/or design failure. Therefore, these breaches were modeled in the risk analysis as having occurred without overtopping. The high water marks (HWM) identified inside the Orleans Basin (where the canal breaches occurred) and the length of time that surge elevations exceeded lake levels in the canals were examined. The HWM during Katrina in the Orleans Basin was within about 1 ft of the peak surge in the canals. For example, it appears that the London Ave. South breach occurred when the canal water level was at about 7 to 8 ft, or about 3 ft below the top of wall. The peak surge in the canal was about 10 to 11 ft, and the HWM in the Orleans Basin was about 10 ft. There was a time lag of several hours between the surge elevation that failed the floodwall and the peak surge elevation. This was a sufficient time period for the water elevation inside the Orleans Basin to reach the peak surge

elevation in the canal. The inverts of the canal breaches were well below the normal lake level, so water flowed back into the lake after the surge passed. Based on these observations, it seemed appropriate to use the peak surge level as the water elevation achieved inside the basin when a catastrophic breach (full levee height) occurred during a non-overtopping event. Therefore, for breaching without overtopping**,** the following assumptions were used in the breaching model**:**

- All breaches were considered to be a result of a structural or foundation failure and the breach depth was set to lowest elevation of the levee or floodwall.
- The breach depth was extended below the adjacent lake or river level.
- The maximum basin water elevations caused by the breach were set to the maximum surge elevation experienced adjacent to the breach.

Breach during an Overtopping Event

For levees subject to overtopping and erosion, general rules were developed that determined breach invert elevation based on the depth of overtopping relative to the top of levee and the type of soil in the levee. In the case where the breach invert elevation was higher than adjacent lake or river levels, the depth and length of the breach, the duration of time that the surge level exceeded the breach invert, and the weir coefficient were required to calculate inflow water volumes for the breach. The breach lengths for the levees were assumed to be similar to that experienced during Katrina. Breach lengths at the major canal breaches varied (450 to 1000+ ft), but were all on the order of several hundred feet. At the industrial canal (IHNC) where overtopping did occur, the two Lower Ninth Ward breaches were similar in length to breaches at canals where overtopping did not occur. The depth of the breaches at canals where overtopping did not occur were below the normal canal water levels; water flowed out through these breaches when the surge passed. Based on these observations, it was assumed that using the peak surge level as the maximum water elevation achieved inside the basin was appropriate when a full-depth breach occurred during an overtopping event.

For the case of a less than full-depth breach given overtopping, breach parameters for width and height were not available for determining inflows. The risk model did not consider breaches that were less than full-depth. This refinement should be added once an erosion model for levees subject to overtopping is available. The risk model only computed full-depth breaches. This approach provided a conservative estimate of basin inflows by assuming a full-depth breach.

The following assumptions were made in the breaching events given overtopping:

- Breaches occurred as a result of an erosion failure due to surge and/or waves.
- All breach depths were assumed to be full levee height; however, the depth of overtopping required to cause a breach was dependent upon soil properties. Assumed values are shown in Table 9-5.
- Durations of overtopping were calculated from the hydrographs.

- The maximum basin water elevations caused by the breach were set to the maximum surge elevation experienced adjacent to the breach.

Table 9-5 Breaching Model

Reaches						
Levee/Floodwall Breach Model Given Overtopping (erosion breach)						
		0 to 1ft		**1ft to 3ft**		
Material	**Symbol**	**Depth (ft)**	**Breach Width (w), Reach Length <1000ft**	**Depth (ft)**	**Breach Width (w) (ft), Reach Length <1000ft**	**Depth (ft)**
Hydraulic Fill	H	0	0	9	0.50*L to max 400	18
Clay	C	0	0	3	0.50*L to max 135	13
Unknown (Average)	U	0	0	6	0.50*L to max 290	17
Wall	W	0	0	0	0	17
		Length Modifiers Reach L>1000 ft				
		Overtopping Depth (ft)				
Material	**Symbol**	**0 to 1ft**		**1ft to 3ft**		**>3 ft**
Hydraulic Fill	H	0.0		400 < w < 0.40*L		430 < w < 0.40*L
Clay	C	0.0		135 < w < 0.10*L		135 < w < 0.10*L
Unknown (Average)	U	0.0		290 < w < 0.30*L		315 < w < 0.30*L
Wall	W	0.0		0.0		315 < w < 0.10*L
Levee/Floodwall Breach Model Given No Overtopping						
			Breach Width (w), (ft)			
Material	**Symbol**	**Depth (ft)**	**L ≤ 1000 ft**	**1000 < L≤ 10,000 ft**	**L>10,000 ft**	**Notes**
Hydraulic Fill	H	18	0.50*L to max 500	500 < w ≤ 0.15*L	0.15*L	3 Breaches / 10,000 reach
Clay	C	13	0.50*L to max 500	500 < w ≤ 0.10*L	0.10*L	2 Breaches / 10,000 reach
Unknown (Average)	U	17	0.50*L to max 500	500 < w ≤ 0.125*L	0.125*L	2.5 Breaches / 10,000 reach
Wall	W	17	0.50*L to max 500	500 < w ≤ 0.075*L	0.075*L	1.5 Breaches / 10,000 reach
Transitions						
Transitions Breach Model Given Overtopping						
		Breach size (ft)				
Transition Type	**Symbol**	**width**	**Depth**			
Ramps	R	25	3			
Floodwall-Levee	T	50	3			
Drainage Structures	D	65	5.5			
Pump Stations	P	100	5			
Gates	G	25	5			
Unprotected sections	U	N/A	N/A			
Transitions Breach Model Given No Overtopping						
		Breach size (ft)				
Transition Type	**Symbol**	**width**	**Depth**			
Ramps	R	-	-	Treated as opened or closed (sand bagged)		
Floodwall-Levee	T	-	-	No breaching until OT		
Drainage Structures	D	-	-	No breaching until OT		
Pump Stations	P	-	-	No breaching until OT		
Gates	G	-	-	Treat as opened or closed		
Unprotected sections	U	N/A	N/A			

Overtopping Volume and Rates

The overtopping rate was computed using the rectangular weir formulae (Daugherty et al. 1985). If the water is assumed to be an ideal liquid, it can be shown using the energy conservation law that the flow rate Q is given by the following equation:

$$Q = \frac{2}{3}(2g)^{1/2} LH^{3/2} \qquad \text{Eq. (9-3)}$$

where g is the acceleration of gravity, H is the water elevation relative to the top of the levee or floodwall, and L is the reach length. The actual flow rate over the weir is known to be less than ideal (Daugherty et al. 1985) because the effective flow area is considerably smaller than the product LH.

The model can be enhanced further for engineering applications by replacing the term $\frac{2}{3}(2g)^{1/2}$ in Eq. 9- 3 by an empirical coefficient, known as the weir coefficient C_w, so that Eq. 9-3 takes on the following form:

$$Q = C_W LH^{3/2} \qquad \text{Eq. (9-4)}$$

where

$$C_W = \begin{cases} 3.33 & \textit{if } L \textit{ and } H \textit{ are given in English units} \\ 1.84 & \textit{if } L \textit{ and } H \textit{ are given in SI units} \end{cases}$$

Note that the C_w for the ideal fluid case is $\frac{2}{3}(2g)^{1/2}$ which is equal to 2.95 m/s^2. This coefficient is assumed to have a coefficient of variation (COV) of 0.2. C_w takes a value of 3.0, 2.6, and 2.0 for floodwalls, levees, and gates, respectively, with a coefficient of variation of 0.2 in English units (L and H in feet).

For the application considered, the mean volume of the overtopping (OT) water μ_V for a given reach can be calculated as

$$\mu_V = C_w L \int \left[\max\left(X_s h_s(t) - H_r, 0\right)\right]^{3/2} dt \qquad \text{Eq. (9-5)}$$

where a hydrograph is represented by $h_s(t)$ as illustrated in Figure 9-7; H_r is the reach height; L is the reach length; C_w is the weir coefficient with a coefficient of variation of 0.2, and a mean $\mu(C_w)$ of 3.0, 2.6, and 2.0 for floodwalls, levees, and gates, respectively; X_s is a random factor

with a lognormal distribution (0.20 log standard deviation and a median of 1.0). The lognormal distribution was applied with the following parameters:

$$\mu = \mathrm{E}(\ln(x)) = 0, \text{ and } \sigma((\ln(x)) = 0.2 \qquad \text{Eq. (9-6)}$$

The resulting volume is the mean volume due to overtopping. The computations account for X_s by numerically using a step size of Δx_{si} and n steps as follows:

$$\mu_{Vi} = \mu_{C_w} L \int_0^{\infty} \left(x_{si} h_s(t) - H_r\right)^{3/2} dt \qquad \text{Eq. (9-7)}$$

where the probability $P(\Delta x_{si})$ can be computed based on the density function f_{X_s} as follows:

$$P(\Delta x_{si}) = \int_{\Delta x_{si}} f_{X_s}(x_s) dx_s \qquad \text{Eq. (9-8)}$$

such that

$$\sum_{i=1}^{n} P(\Delta x_{si}) = \sum_{i=1}^{n} \int_{\Delta x_{si}} f_{X_s}(x_s) dx_s = 1 \qquad \text{Eq. (9-9)}$$

For each hurricane, the event tree was evaluated n times, and the branch probabilities for these evaluations were multiplied by the respective $P(\Delta x_{si})$ according to Eq. 9-9. This step resulted in the number of branches produces being multiplied by n.

The variance of the water volume for each case was computed based on the coefficient of variation (δ) of the weir coefficient as follows:

$$\sigma_{Vi}^2 = (\mu_{Vi} \delta_{Cw})^2 \qquad \text{Eq. (9-10)}$$

where μ_{Vi} is provided by Eq. 9-7, and the coefficient of variation (δ) of the weir coefficient is taken as 0.2.

Failure and Overtopping Probability

The cumulative distribution function (CDF) of the total water volume contained in a subbasin of n reaches was computed as follows:

$$F_V = \sum_{i=1}^{n} p_i F_{V_i} \qquad \text{Eq. (9-11)}$$

where p_i = a overtopping probability, and F_V = CDF of the total water volume. The overtopping probability was treated as a binary variable. For the case of point estimates of flooding per reach, computations were based on order statistics. Once the total volume was obtained from all overtopping and breach cases, the net volume (as a random variable) was computed by adding (or subtracting) water volumes from rainfall, wave runup and the effect of pumping.

Event Tree Branch Probabilities

The event tree of Figure 9-8 consists of 12 branches per hurricane. This section develops and summarizes the probabilities for these branches.

The event tree includes the following primary independent sub-basin-level events:

- *C* is the event that all gates within a sub-basin are closed,
- *P* is the event that all pumps in the sub-basin work, and
- *B* is the event that at least one reach (or one of its transition features) in a sub-basin is breached.

These events were used to construct Table 9-6 that summarizes the expanded expressions for the probability of each branch in the event tree of Figure 9-8. Table 9-7 summarizes the respective procedures for water volume and elevation computation. It should be noted that the water volume associated with the branches involving *not-all-gates closed* required a procedure to account for all possible combinations of not-all-gates closed. Let *i* be the index denoting a unique scenario among the set of 2^n scenarios of gate open/closed combinations (n = number of uncorrelated gates). The mean water volume (μ) used in the not-all-gates closed branches was:

$$\mu_{\underline{C}} = \frac{\sum_{i=1}^{2^n} p_i \mu_{\underline{C}i}}{(1 - p_C)} \qquad \text{Eq. (9-12)}$$

where p_C is the probability of all gates closed, $\mu_{\underline{C}i}$ the mean volume associated with not-closing gates according to the i^{th} scenario, and p_i the multinomial probability of the i^{th} scenario. The volume variance used in the not-all-gates closed branches was:

$$\sigma^2_{\underline{C}} = \frac{\sum_{i=1}^{2^n} p_i^2 \sigma^2_{\underline{C}i}}{(1 - p_C)^2} \qquad \text{Eq. (9-13)}$$

where $\sigma^2_{\underline{C}i}$ is the volume variance associated with not-closing gates according to the i^{th} scenario.

The subbasin interflow analysis as previously described was performed subsequent to Table 9-6 procedures. Water volumes were converted to elevations with a tabulated stage-storage relationship for each subbasin based on linear interpolation. Uncertainty propagation from the volume (V) moments (μ_V and σ_V^2) to elevation (E) moments (μ_E and σ_E^2) also used the tabulated stage-storage relationship. Linear interpolation was used since the stage-storage data was tabulated in increments of 1 ft.

The results produced at this point were summarized by subbasin, for all storms and branches of the event tree, in the form of water elevation (mean and variance) and occurrence rate. These results were used to estimate an elevation-exceedance rate for a subbasin at selected elevation (e) values as follows:

$$\lambda\left(E > e\right) = \sum_{All\ storms\ \&\ branches} \lambda P\left(h\right) P\left(S \mid h\right) P\left(E > e \mid h, S\right) \qquad \text{Eq. (9-14)}$$

This linear relationship can be expressed as

$$E = a + bV \qquad \text{Eq. (9-15)}$$

where coefficients a and b were determined from interpolation. The moments of E were computed as

$$\mu_E = a + b\mu_V \qquad \text{Eq. (9-16)}$$

and

$$\sigma_E^2 = b^2\sigma_V^2 \qquad \text{Eq. (9-17)}$$

Table 9- 6
A Computational Summary for Branches of the Event Tree of Figure 9- 6 for a Hurricane and a Basin

Branch	Branch Probability (See Figure 9-6)
1. Non-Breach	$P(C)P(P)P(\underline{B}\cap\underline{O}) = P(C)P(P)\left(\prod_i (1-P_i(B\mid\underline{O}))P_i(\underline{O})\right)$
2. Non-Breach	$P(C)P(\underline{P})P(\underline{B}\cap\underline{O}) = P(C)P(\underline{P})\left(\prod_i (1-P_i(B\mid\underline{O}))P_i(\underline{O})\right)$
3. Breach	$P(C)P(B\cap\underline{O}) = P(C)\left(1-\left(\prod_i (1-P_i(B\mid\underline{O}))P_i(\underline{O})\right)\right)$
4. Non-Breach	$P(C)P(P)P(\underline{B}\cap O) = P(C)P(P)\left(P(\underline{B})-P(\underline{B}\cap\underline{O})\right) =$ $P(C)P(P)\left(\prod_i \left((1-P_i(B\mid O))P_i(O)+(1-P_i(B\mid\underline{O}))P_i(\underline{O})\right)-\prod_i (1-P_i(B\mid\underline{O}))P_i(\underline{O})\right)$
5. Non-Breach	$P(C)P(\underline{P})P(\underline{B}\cap O) = P(C)P(P)\left(P(\underline{B})-P(\underline{B}\cap\underline{O})\right) =$ $P(C)P(\underline{P})\left(\prod_i \left((1-P_i(B\mid O))P_i(O)+(1-P_i(B\mid\underline{O}))P_i(\underline{O})\right)-\prod_i (1-P_i(B\mid\underline{O}))P_i(\underline{O})\right)$
6. Breach	$P(C)P(B\cap O) = P(C)\left(1-P(\underline{B})-P(\underline{B}\cap\underline{O})\right) =$ $P(C)\left(1-\prod_i \left((1-P_i(B\mid O))P_i(O)+(1-P_i(B\mid\underline{O}))P_i(\underline{O})\right)-\prod_i (1-P_i(B\mid\underline{O}))P_i(\underline{O})\right)$
7. Non-Breach	$(1-P(C))P(P)P(\underline{B}\cap\underline{O}) = (1-P(C))P(P)\left(\prod_i (1-P_i(B\mid\underline{O}))P_i(\underline{O})\right)$
8. Non-Breach	$(1-P(C))P(\underline{P})P(\underline{B}\cap\underline{O}) = (1-P(C))P(\underline{P})\left(\prod_i (1-P_i(B\mid\underline{O}))P_i(\underline{O})\right)$
m9. Breach	$(1-P(C))P(B\cap\underline{O}) = (1-P(C))\left(1-\left(\prod_i (1-P_i(B\mid\underline{O}))P_i(\underline{O})\right)\right)$
10. Non-Breach	$(1-P(C))P(P)P(\underline{B}\cap O) = P(C)P(P)\left(P(\underline{B})-P(\underline{B}\cap\underline{O})\right) =$ $(1-P(C))P(P)\left(\prod_i \left((1-P_i(B\mid O))P_i(O)+(1-P_i(B\mid\underline{O}))P_i(\underline{O})\right)-\prod_i (1-P_i(B\mid\underline{O}))P_i(\underline{O})\right)$
11. Non-Breach	$(1-P(C))P(\underline{P})P(\underline{B}\cap O) = P(C)P(P)\left(P(\underline{B})-P(\underline{B}\cap\underline{O})\right) =$ $(1-P(C))P(\underline{P})\left(\prod_i \left((1-P_i(B\mid O))P_i(O)+(1-P_i(B\mid\underline{O}))P_i(\underline{O})\right)-\prod_i (1-P_i(B\mid\underline{O}))P_i(\underline{O})\right)$
12. Breach	$(1-P(C))P(B\cap O) = P(C)\left(1-P(\underline{B})-P(\underline{B}\cap\underline{O})\right) =$ $(1-P(C))\left(1-\prod_i \left((1-P_i(B\mid O))P_i(O)+(1-P_i(B\mid\underline{O}))P_i(\underline{O})\right)-\prod_i (1-P_i(B\mid\underline{O}))P_i(\underline{O})\right)$
Combined Branches 3 and 9	$\left(P(C)+P(\underline{C})\right)\left(P(P)+P(\underline{P})\right)(B\cap\underline{O}) = 1-\left(\prod_i (1-P_i(B\mid\underline{O}))P_i(\underline{O})\right)$
Combined Branches 6 and 12	$\left(P(C)+P(\underline{C})\right)\left(P(P)+P(\underline{P})\right)\left(1-P(\underline{B})-P(\underline{B}\cap\underline{O})\right) =$ $1-\prod_i \left((1-P_i(B\mid O))P_i(O)+(1-P_i(B\mid\underline{O}))P_i(\underline{O})\right)-\prod_i (1-P_i(B\mid\underline{O}))P_i(\underline{O})$

Table 9- 7
A Computational Summary for the Water Volumes Associated with the Branches of the Event Tree of Figure 9- 6 for a Hurricane and a Basin

Branch	Branch Water Volume (See Figure 9- 6)
1. Non-Breach	Use precipitation volume, and apply pumping factor
2. Non-Breach	Use precipitation volume without pumping
3. Breach	Use post-surge breach water elevation, no pumping
4. Non-Breach	Use overtopping and precipitation volume, apply pumping factor
5. Non-Breach	Use overtopping and precipitation volume without pumping
6. Breach	Use post-surge breach water elevation, no pumping
7. Non-Breach	Use precipitation and not-all-closed-closure volume apply pumping factor
8. Non-Breach	Use precipitation and not-all-closed-closure volume without pumping
9. Breach	Use post-surge breach water elevation, no pumping
10. Non-Breach	Use overtopping, precipitation and not-all-closed-closure volume apply pumping factor
11. Non-Breach	Use overtopping, precipitation and not-all-closed-closure volume without pumping
12. Breach	Use post-surge breach water elevation, no pumping

Risk Profiles

The construction of risk profiles required that all storms be evaluated for all possible combinations of events (all event tree branches) for all the basins. The number of combination per storm for eight basins and 12 branches of the event tree was 1,073,741,824. Dependency among the basins was not examined in order to reduce the number of possible combinations; however, the risk results obtained by examining the individual basins were considered adequate for evaluating the relative risks and vulnerabilities of the HPS.

By Water Elevation

Forte results were summarized by sub-basin, for all storms and the branches of the event tree in the form of water elevation (mean and variance) and occurrence rate. These results were used to evaluate elevation-exceedance rates for a subbasin at selected elevation *e* values according to Eq. 9-18 as follows:

$$\lambda(E > e) = \sum_{All\ storms\ \&\ branches} \lambda P(h) P(S \mid h) P(E > e \mid h, S) \tag{9-18}$$

An example of an elevation exceedance curve is shown in Figure 9-11. Given elevation-exceedance probabilities and hurricane occurrence rates for a subbasin, and considering all storms, flood water inundation maps were developed as illustrated in Figure 9-12. The inundation maps show the return periods corresponding to respective elevations.

Forte conducted interflow analyses between subbasins at the basin level for individual storms. The Forte analyses did not include overtopping water volumes due to wave runup,

pumping, or interflow analyses at the basin level when the storms were aggregated. For each basin, these volumes were added to the Forte water volumes using deterministic calculations. Three states of pumping system effectiveness were considered: no pumping, pumping at 50 percent of capacity, and at 100 percent of capacity. The basin analyses modified the final 50, 100, and 500 year sub-basin elevations by adding wave run-up overtopping volumes and by subtracting the averaged value for pumping volume expected over the entire storm set. Pumping volumes were estimated deterministically based on each storm's duration and intensity within each sub-basin, averaged over the set of storms, and subtracted from the 50, 100 and 500-yr elevations using the stage-storage relationship for each sub-basin.

After modifying the basin water volumes due to wave runup and pumping, the Forte results at the 50, 100 and 500 year exceedance rates were examined and balanced at a basin level by looking at the water volumes produced at each exceedance level using the stage-storage relationships for the sub-basins. If the interflow elevations between subbasins were exceeded, water volumes were redistributed and new water surface elevations were determined. Note that the exceedance rates were conditional on the storm set provided to the risk team with frequencies as shown in Appendix 8 which do not consider tropical storms and lower intensity, more frequent hurricanes. The actual inundation maps developed from the final results of the risk analysis are shown in Appendix 13.

By Economic and Life losses

Using the elevation-exceedance curve, economic and life loss profiles were estimated and results were provided as elevation-loss curves per sub-basins. The risk profiles for the HPS are expressed in terms of the life loss consequences (as illustrated in Figure 9-13) and the direct economic (as illustrated by Figure 9-14) based upon the stage-damage curves. The stage-damage curves used to construct these profiles were provided by the IPET Consequence Team. The life and economic risk profiles developed from the final results of the risk analysis are shown in Appendix 13.

Conclusions and Recommendations

In developing the risk analysis methodology for the New Orleans hurricane protection system, the needs of decision and policy makers led to the requirements of producing an analytic, transparent, defensible, quantitative, probabilistic, and consistent methodology. Quantifying risk using a probabilistic framework produced elevation and loss exceedance rates based on a spectrum of hurricanes according the joint probability distribution of the characteristic parameters that define hurricane intensity and the resulting surges, waves and precipitation. The methodology provides a process for evaluating the performance of a hurricane protection systems consisting of levees, floodwalls, transitions, closure gates, drainage systems and pumping stations, and estimates the population and property at risk by considering the best estimate flood levels of each basin for occurrence rates of 0.02, 0.01, and 0.002 (i.e., average return periods of 50 years, 100 years, and 500 years). The quantification of risk will assist decision makers as they consider various alternatives to manage risk through the enhancement of the hurricane protection system, controlling land use, improving evacuation effectiveness, and

improving drainage system operations. It also provides public and private stakeholders with information that can be used to increase hurricane preparedness and the awareness of the risks associated with living in a hurricane prone environment.

References

ADCIRC, 2006. Finite Element Hydrodynamic Model for Coastal Oceans, Inlets, Rivers and Floodplains, *http://www.nd.edu/~adcirc/index.htm*.

Ayyub, B. M. 2003. Risk Analysis in Engineering and Economics, Chapman & Hall/CRC Press, FL.

Ayyub, B. M., and McCuen, R. H. 2003. Probability, Statistics and Reliability for Engineers and Scientists, Chapman & Hall/CRC Press, FL.

Daugherty, R., Franzini, J., and Finnemore E., 1985, Fluid Mechanics with Engineering Applications, 598 p., McGraw-Hill Book Co., NY.

Dixon, T. H., Amelung, F., and Ferretti, A.. 2006. "Subsidence and Flooding in New Orleans," Nature 441, 587-588.

Dokka, R. K., 2006. "Modern-Day Tectonic Subsidence in Coastal Louisiana," Geology 34(4), 281–284.

Eijgenraam, C. J. J., 2006. Optimal Safety Standards for Dike-Ring Areas. CPB Netherlands Bureau for Economic Policy Analysis: CPB Discussion Paper 62.

Federal Emergency Management Agency (FEMA), 2006. Mitigation Assessment Team Report: Hurricane Katrina in the Gulf Coast - Building Performance Observations, Recommendations, and Technical Guidance (July 2006). http://www.fema.gov/library/viewRecord.do?id=1857

Grossi, P. and Kunreuther, H., 2005. Catastrophe Modeling: A New Approach to Managing Risk. Springer-Verlag, New York.

Holland, G. J., 1980. "An Analytic Model of the Wind and Pressure Profiles in Hurricanes." Monthly Weather Review, 108, 1212-1218.

Kumamoto, H., and Henley, E.J., 1996, Probabilistic Risk Assessment and Management for Engineers and Scientists, Second Edition, IEEE Press, New York.

McGill, W. L., Ayyub, B. M., Kaminskiy, M., "Risk Analysis for Critical Asset Protection,"

Risk Analysis, Society for Risk Analysis, (accepted for publication).

Modarres, M., Kaminskiy, M., Krivstov, V., 1999. Reliability Engineering and Risk Analysis: A Practical Guide, Marcel Decker Inc., New York, NY.

Muir-Wood, R. and Bateman, W., 2005. "Uncertainties and Constraints on Breaching and Their Implications for Flood Loss Estimation." Philosophical Transactions of the Royal Society A: Mathematical, Physical, and Engineering Sciences, 363(1831), 1423-1430.

National Flood Insurance Program (NFIP), 2006. Flood Insurance Manual: May 2005 (Revised October 2006). http://www.fema.gov/business/nfip/manual200610.shtm

US Senate, 2006. Hurricane Katrina: A Nation Still Unprepared, Report to the Committee on Homeland Security and Government Affairs, US Senate, Washington, DC. USACE, 2006. Interagency Performance Evaluation Task Force Draft Report on "Performance Evaluation of the New Orleans and Southeast Louisiana Hurricane Protection System," Draft Volume VIII – Engineering and Operational Risk and Reliability Analysis, USACE, Washington, DC. (1 June 2006). *https://IPET.wes.army.mil*

Van Gelder, M., 2000. Statistical Methods for Risk-based Design of Civil Structures, PhD Thesis, Delft University of Technology, Report No. 00-1, The Netherlands.

Van Manen, S. E., Brinkhuis, M. 2005. "Quantitative Flood Risk Assessment for Polders." Reliability Engineering & System Safety, 90, 229-237.

Voortman, H., 2003. Risk-based Design of Large Scale Flood Defence Systems, PhD Thesis, Delft University of Technology, Report No. 02-3, The Netherlands.

White House, 2006. The Federal Response to Hurricane Katrina: Lessons Learned. *http://www.whitehouse.gov/reports/katrina-lessons-learned/*

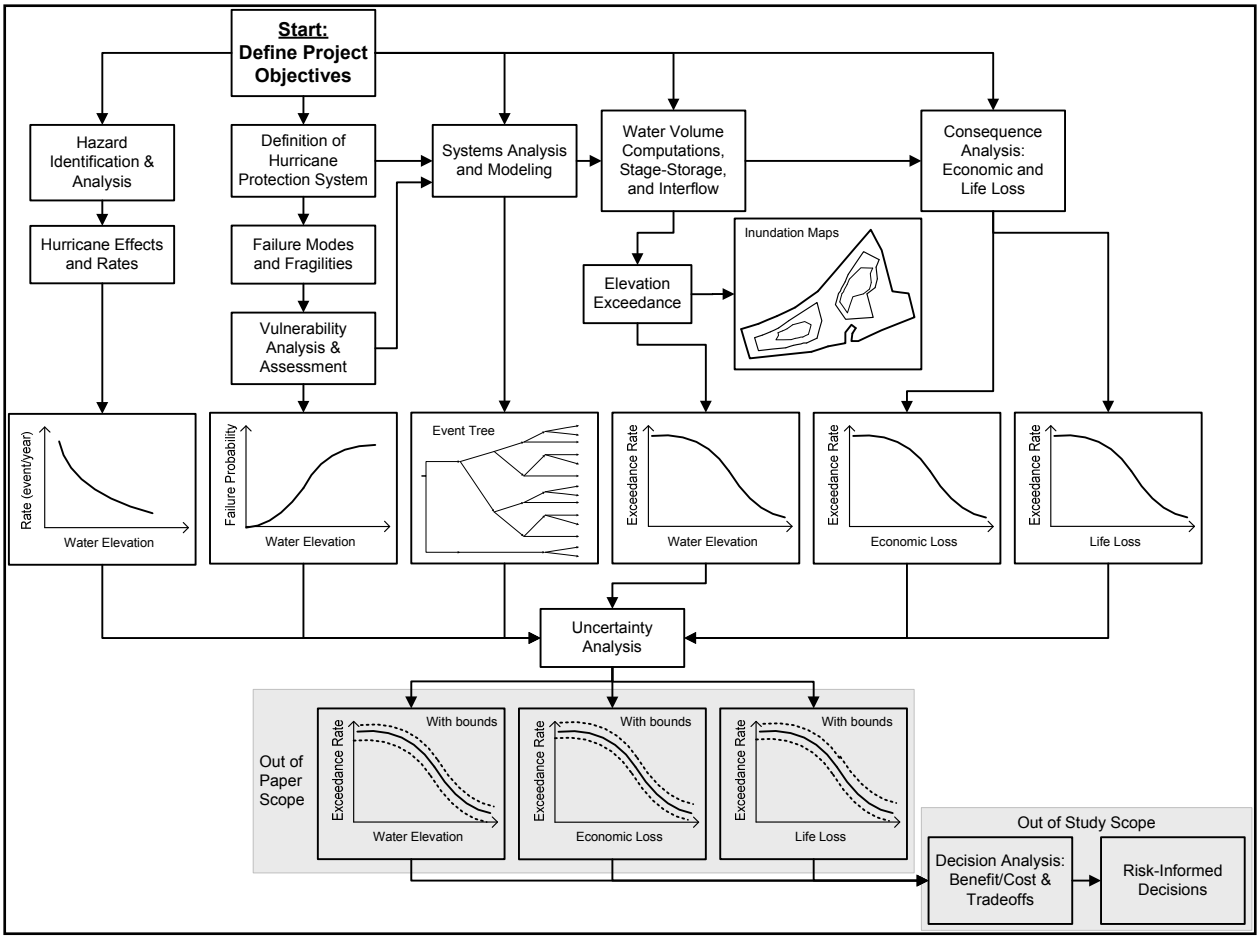

Figure 9-1. Risk Analysis Logic Diagram

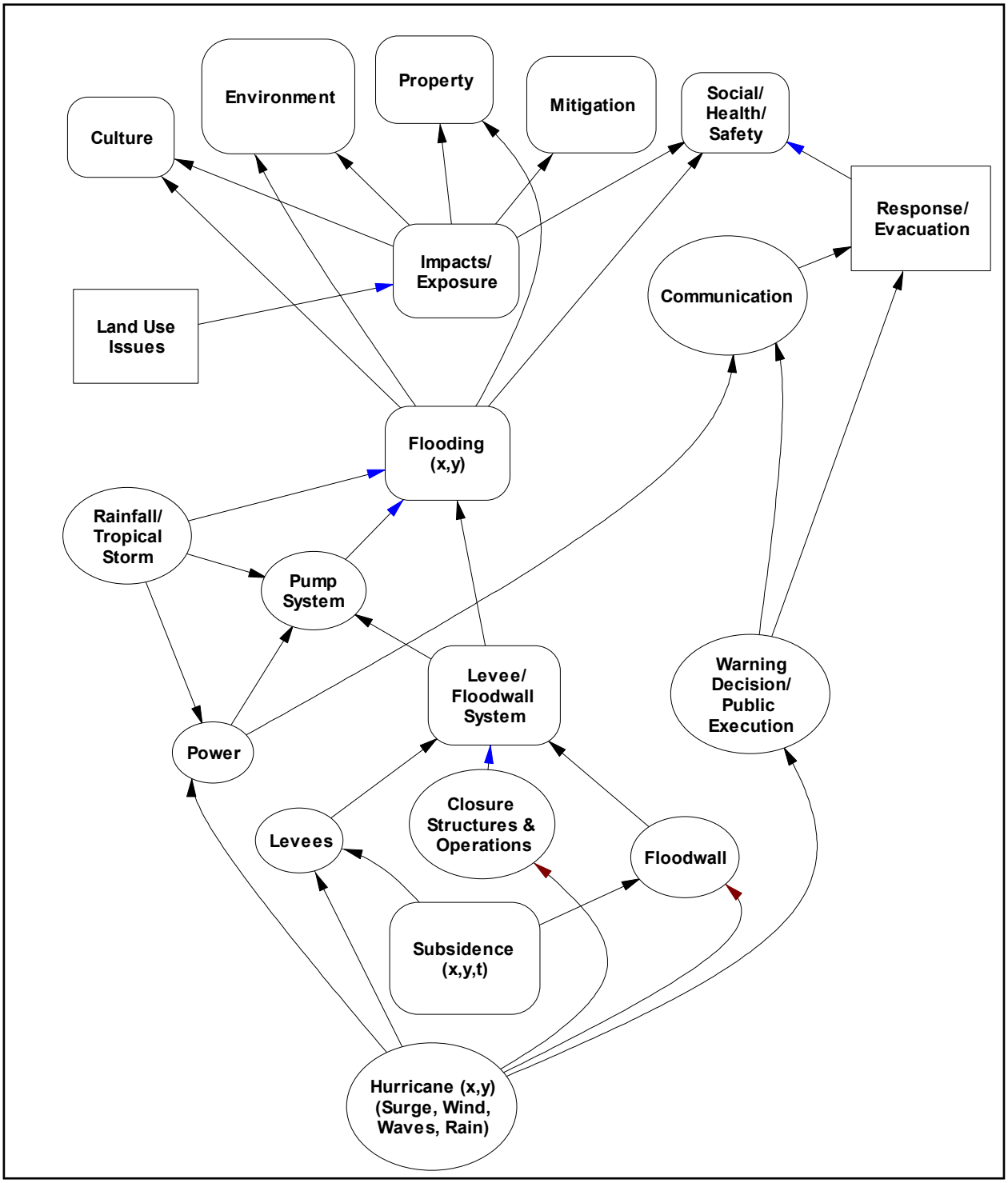

Figure 9-2. Influence Diagrams for Risk Analysis

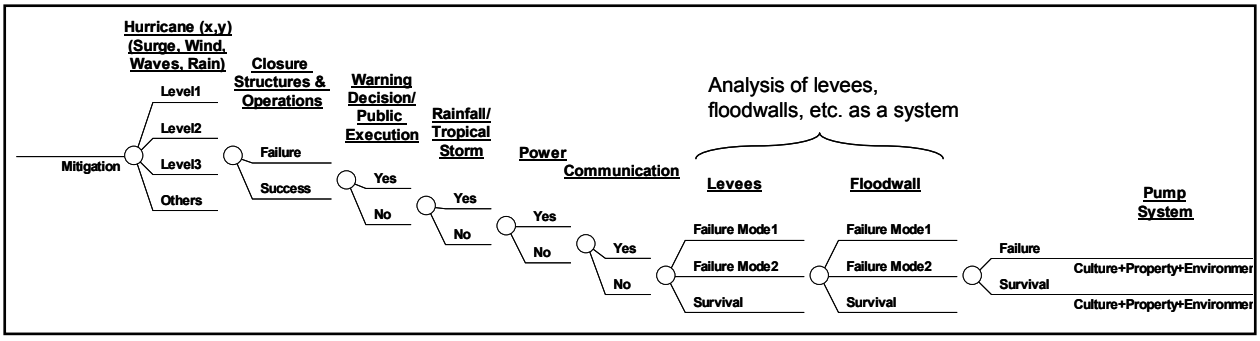

Figure 9- 3. Probability Tree for the Hurricane Protection System

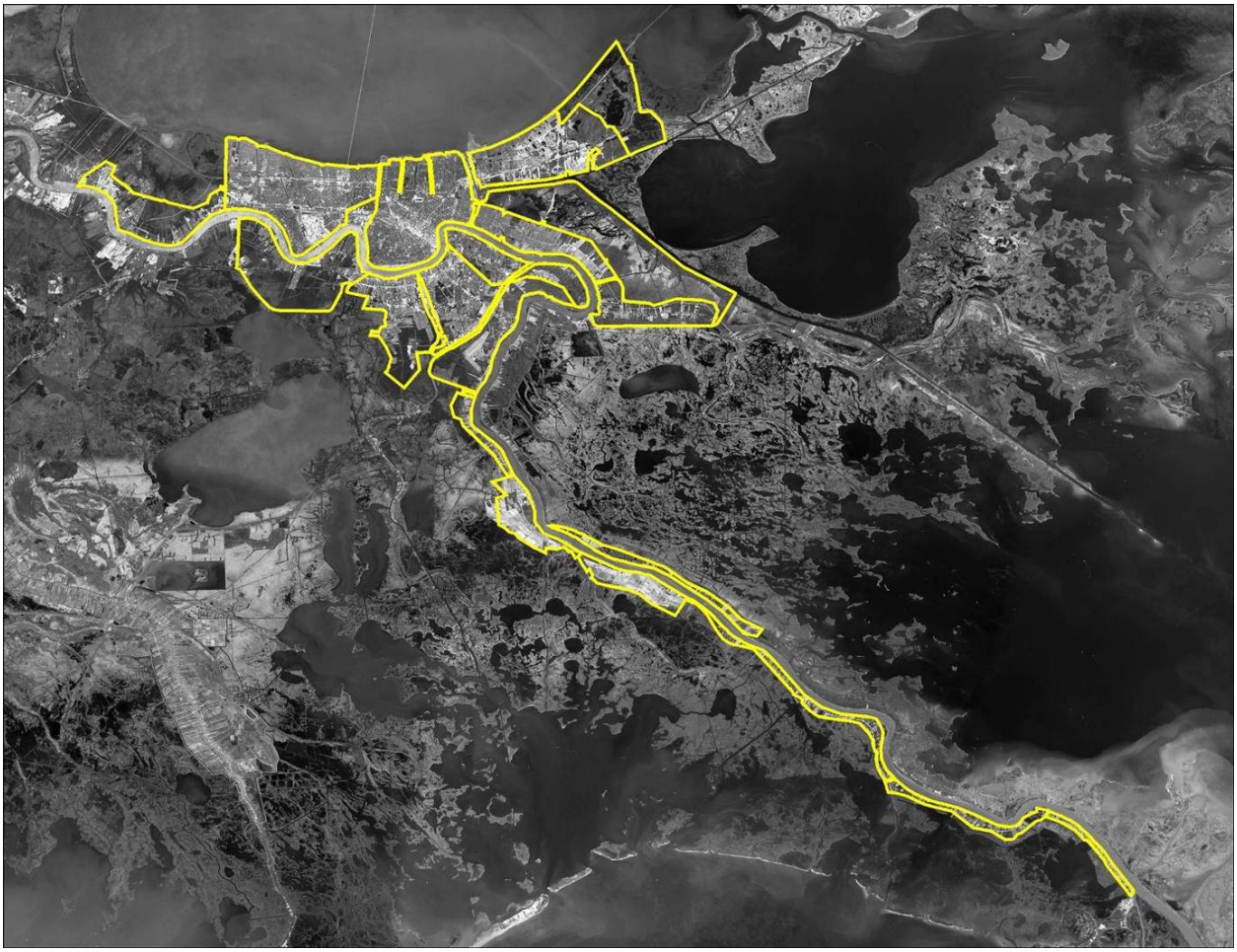

Figure 9-4. Map of New Orleans and the South East Louisiana Area Showing the Geographic Bounds of the Study Region Considered in the Risk Analysis

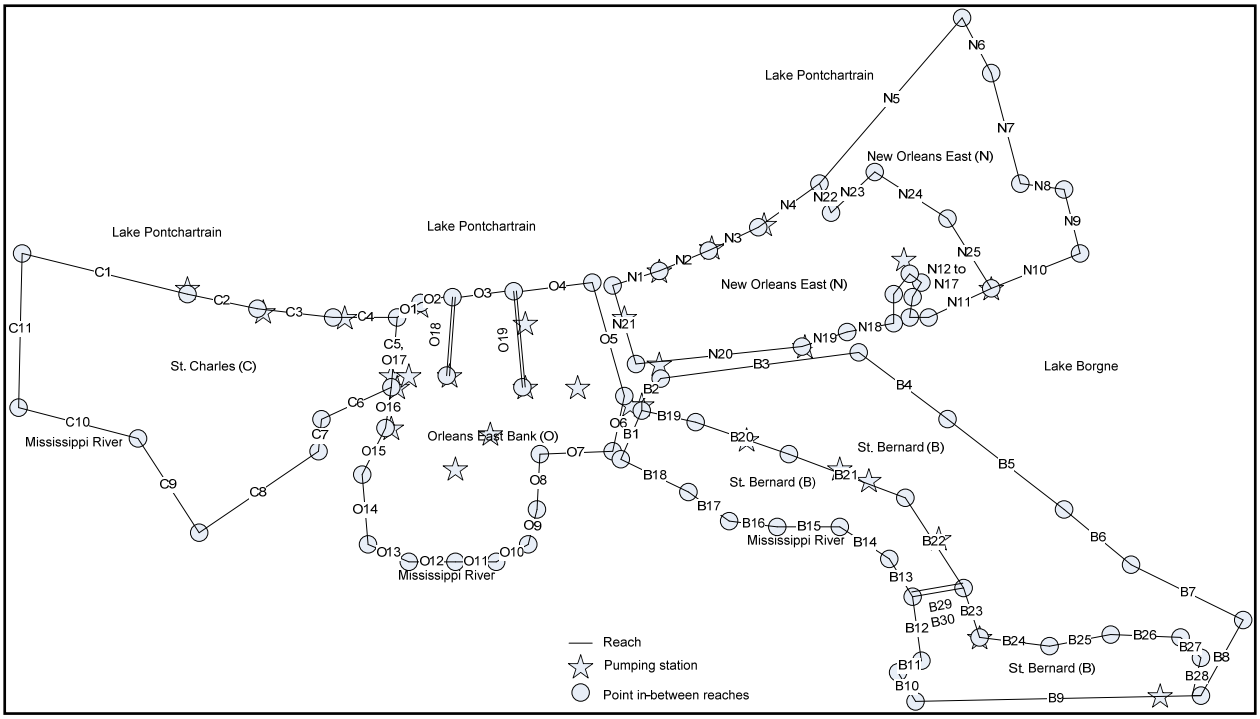

Figure 9- 5. Hurricane Protection System Defined by Basins and Reaches

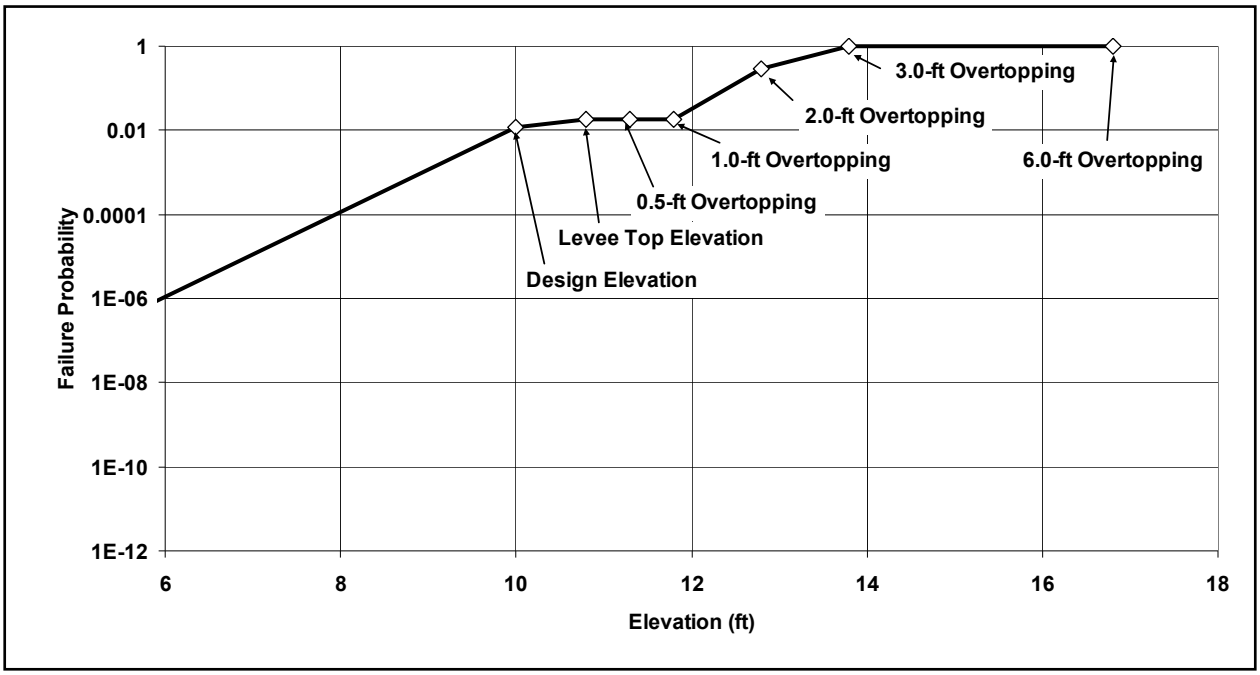

Figure 9-6 Example of a Fragility Curve

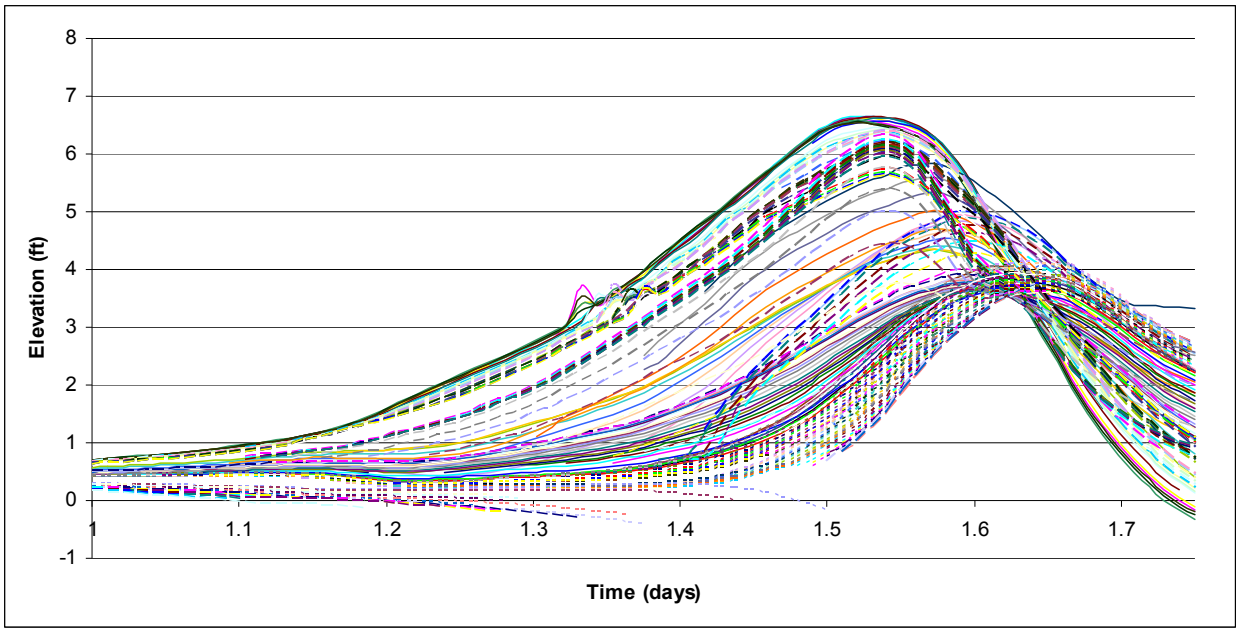

Figure 9-7. Hydrographs of Storm Surge at Defined Stations in the Hurricane Protection System for a Single Storm Event.

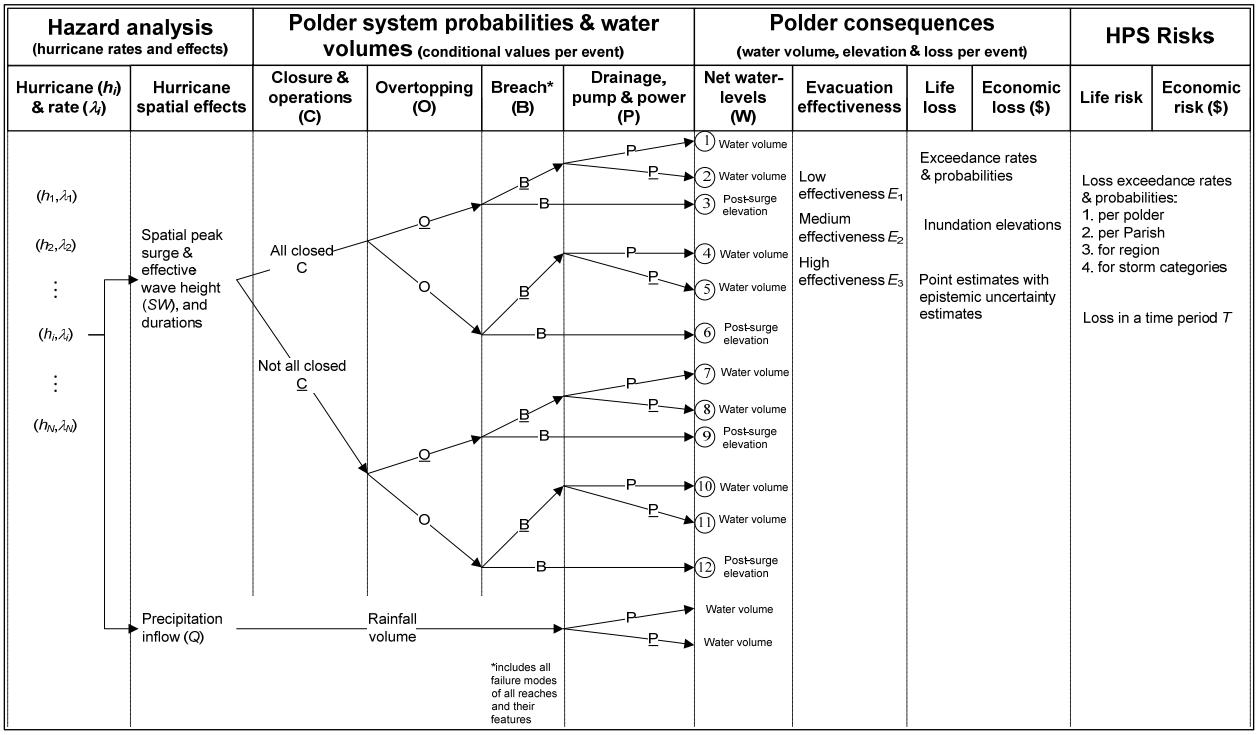

Figure 9-8. Event Tree for Quantifying Risk.

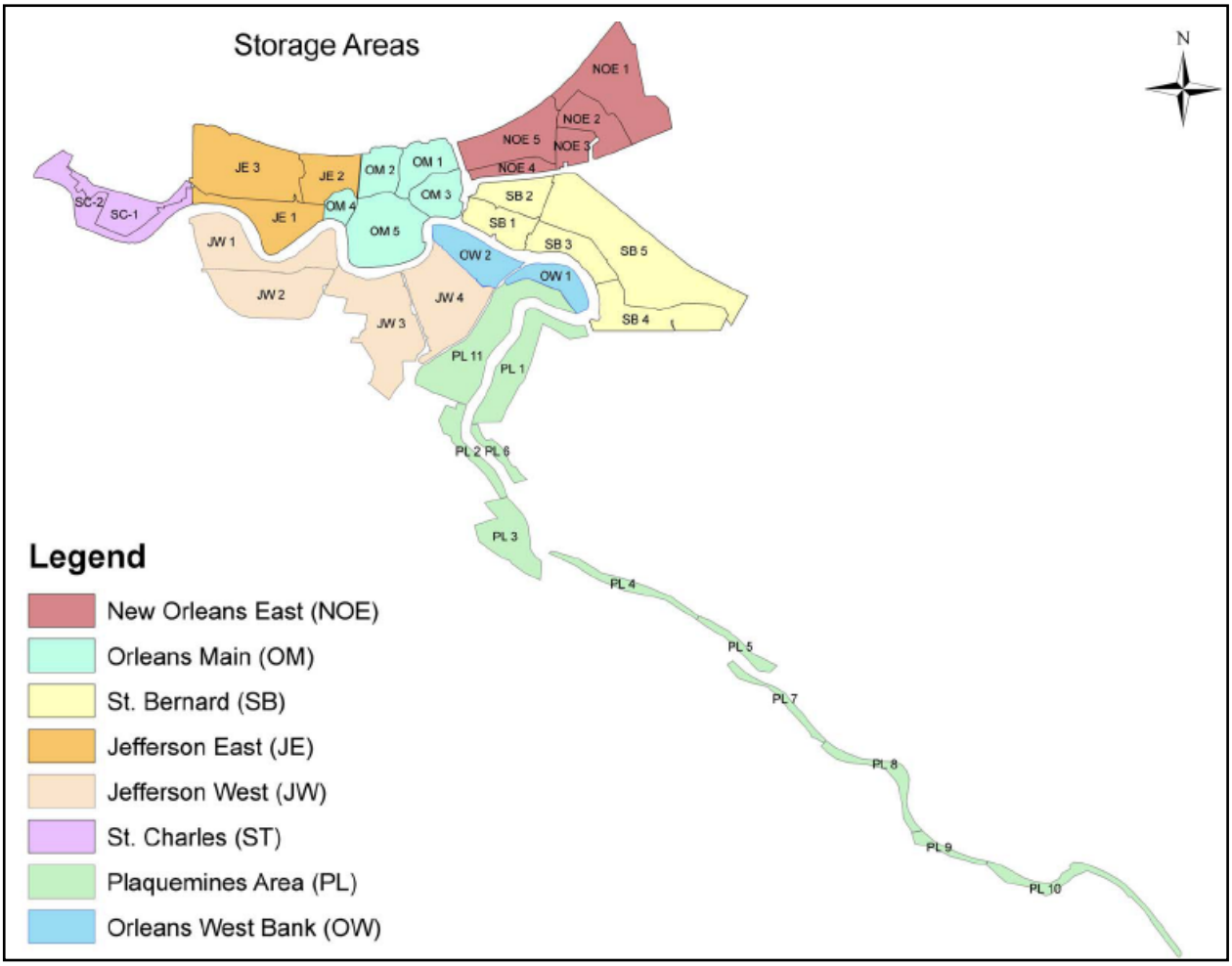

Figure 9-9. Definition of Sub basins for New Orleans HPS.

Figure 9-10. Typical Stage-Storage Curve

Table 9-3
Storm Frequencies and Parameters

Sequential number - IPET R&R Storm	Storm Frequency (Events/yr)	Central pressure deficit at landfall (P0)	Radius to maximum winds at landfall (Rp)	Forward speed at landfall (Vf) (Mph)	Holland's parameter (B)	Track angle at landfall wrt vertical (A)	Track Identifer	Lat	Long
1	7.90E-04	960	11	11	1.27	0	1	24.43	-79.1
2	9.19E-04	960	21	11	1.27	0	1	24.43	-79.1
3	4.92E-04	960	35.6	11	1.27	0	1	24.43	-79.1
4	2.50E-03	930	8	11	1.27	0	1	24.43	-79.1
5	2.73E-03	930	17.7	11	1.27	0	1	24.43	-79.1
6	2.30E-03	930	25.8	11	1.27	0	1	24.43	-79.1
7	1.13E-03	900	6	11	1.27	0	1	24.43	-79.1
8	1.39E-03	900	14.9	11	1.27	0	1	24.43	-79.1
9	3.46E-04	900	21.8	11	1.27	0	1	24.43	-79.1
10	7.90E-04	960	11	11	1.27	0	2	24.42	-78.6
11	9.19E-04	960	21	11	1.27	0	2	24.42	-78.6
12	4.92E-04	960	35.6	11	1.27	0	2	24.42	-78.6
13	2.50E-03	930	8	11	1.27	0	2	24.42	-78.6
14	2.73E-03	930	17.7	11	1.27	0	2	24.42	-78.6
15	2.30E-03	930	25.8	11	1.27	0	2	24.42	-78.6
16	1.13E-03	900	6	11	1.27	0	2	24.42	-78.6
17	1.39E-03	900	14.9	11	1.27	0	2	24.42	-78.6
18	3.46E-04	900	21.8	11	1.27	0	2	24.42	-78.6
19	7.90E-04	960	11	11	1.27	0	3	24.42	-78.5
20	9.19E-04	960	21	11	1.27	0	3	24.42	-78.5
21	4.92E-04	960	35.6	11	1.27	0	3	24.42	-78.5
22	2.50E-03	930	8	11	1.27	0	3	24.42	-78.5
23	2.73E-03	930	17.7	11	1.27	0	3	24.42	-78.5
24	2.30E-03	930	25.8	11	1.27	0	3	24.42	-78.5
25	1.13E-03	900	6	11	1.27	0	3	24.42	-78.5
26	1.39E-03	900	14.9	11	1.27	0	3	24.42	-78.5
27	3.46E-04	900	21.8	11	1.27	0	3	24.42	-78.5
28	7.90E-04	960	11	11	1.27	0	4	24.4	-77.9
29	9.19E-04	960	21	11	1.27	0	4	24.4	-77.9
30	4.92E-04	960	35.6	11	1.27	0	4	24.4	-77.9
31	2.50E-03	930	8	11	1.27	0	4	24.4	-77.9
32	2.73E-03	930	17.7	11	1.27	0	4	24.4	-77.9
33	2.30E-03	930	25.8	11	1.27	0	4	24.4	-77.9
34	1.13E-03	900	6	11	1.27	0	4	24.4	-77.9
35	1.39E-03	900	14.9	11	1.27	0	4	24.4	-77.9
36	3.46E-04	900	21.8	11	1.27	0	4	24.4	-77.9
37	7.90E-04	960	11	11	1.27	0	5	24.43	-78.9
38	9.19E-04	960	21	11	1.27	0	5	24.43	-78.9
39	4.92E-04	960	35.6	11	1.27	0	5	24.43	-78.9
40	2.50E-03	930	8	11	1.27	0	5	24.43	-78.9
41	2.73E-03	930	17.7	11	1.27	0	5	24.43	-78.9
42	2.30E-03	930	25.8	11	1.27	0	5	24.43	-78.9

43	1.13E-03	900	6	11	1.27	0	5	24.43	-78.9
44	1.39E-03	900	14.9	11	1.27	0	5	24.43	-78.9
45	3.46E-04	900	21.8	11	1.27	0	5	24.43	-78.9
46	3.50E-04	960	18.2	11	1.27	-45	1	24.54	-80.9
47	3.90E-04	960	24.6	11	1.27	-45	1	24.54	-80.9
48	7.16E-04	900	12.5	11	1.27	-45	1	24.54	-80.9
49	5.48E-04	900	18.4	11	1.27	-45	1	24.54	-80.9
50	3.50E-04	960	18.2	11	1.27	-45	2	24.83	-80.8
51	3.90E-04	960	24.6	11	1.27	-45	2	24.83	-80.8
52	7.16E-04	900	12.5	11	1.27	-45	2	24.83	-80.8
53	5.48E-04	900	18.4	11	1.27	-45	2	24.83	-80.8
54	3.50E-04	960	18.2	11	1.27	-45	3	25.38	-80.8
55	3.90E-04	960	24.6	11	1.27	-45	3	25.38	-80.8
56	7.16E-04	900	12.5	11	1.27	-45	3	25.38	-80.8
57	5.48E-04	900	18.4	11	1.27	-45	3	25.38	-80.8
58	3.50E-04	960	18.2	11	1.27	-45	4.1	26.08	-80.8
59	3.90E-04	960	24.6	11	1.27	-45	4.1	26.08	-80.8
60	7.16E-04	900	12.5	11	1.27	-45	4.1	26.08	-80.8
61	5.48E-04	900	18.4	11	1.27	-45	4.1	26.08	-80.8
63	2.50E-04	960	24.6	11	1.27	45	1	21.28	-90
64	3.02E-04	900	12.5	11	1.27	45	1	21.28	-90
65	2.01E-04	900	18.4	11	1.27	45	1	21.28	-90
66	1.54E-04	960	18.2	11	1.27	45	2	21.3	-90
67	2.50E-04	960	24.6	11	1.27	45	2	21.3	-90
68	3.02E-04	900	12.5	11	1.27	45	2	21.3	-90
69	2.01E-04	900	18.4	11	1.27	45	2	21.3	-90
70	1.54E-04	960	18.2	11	1.27	45	3	21.27	-90.1
71	2.50E-04	960	24.6	11	1.27	45	3	21.27	-90.1
72	3.02E-04	900	12.5	11	1.27	45	3	21.27	-90.1
73	2.01E-04	900	18.4	11	1.27	45	3	21.27	-90.1
74	1.54E-04	960	18.2	11	1.27	45	4	21.28	-90
75	2.50E-04	960	24.6	11	1.27	45	4	21.28	-90
76	3.02E-04	900	12.5	11	1.27	45	4	21.28	-90
77	2.01E-04	900	18.4	11	1.27	45	4	21.28	-90
Total	7.45E-02								
62		960	18.2	11	1.27	45	1	21.28	-90
78		960	17.7	6	1.27	0	1	24.43	-78.9
79		900	17.7	6	1.27	0	1	24.43	-78.9
80		960	17.7	6	1.27	0	2	24.42	-78.4
81		900	17.7	6	1.27	0	2	24.42	-78.4
82		960	17.7	6	1.27	0	3	24.42	-78.3
83		900	17.7	6	1.27	0	3	24.42	-78.3
84		960	17.7	6	1.27	0	4	24.4	-77.7
85		900	17.7	6	1.27	0	4	24.4	-77.7
86		960	17.7	6	1.27	0	5	24.42	-78.7
87		900	17.7	6	1.27	0	5	24.42	-78.7
88		930	17.7	6	1.27	-45	1	26.94	-80.9
89		930	17.7	6	1.27	-45	2	27.09	-80.9
90		930	17.7	6	1.27	-45	3	27.52	-80.9

91		930	17.7	6	1.27	-45	4.1	28.21	-80.9
92		930	17.7	6	1.27	45	1	20.66	-92.3
93		930	17.7	6	1.27	45	2	20.75	-92.6
94		930	17.7	6	1.27	45	3	20.91	-92.8
95		930	17.7	6	1.27	45	4	21.17	-93
96		930	17.7	17	1.27	0	1	24.43	-79.1
97		930	17.7	17	1.27	0	2	24.42	-78.6
98		930	17.7	17	1.27	0	3	24.42	-78.5
99		930	17.7	17	1.27	0	4	24.4	-77.8
100		930	17.7	17	1.27	0	5	24.43	-78.9
101		930	17.7	17	1.27	-45	1	23.29	-80.8
102		930	17.7	17	1.27	-45	2	23.68	-80.9
103		930	17.7	17	1.27	-45	3	24.27	-80.8
104		930	17.7	17	1.27	-45	4.1	24.94	-80.7
105		930	17.7	17	1.27	45	1	21.28	-90
106		930	17.7	17	1.27	45	2	21.27	-90.1
107		930	17.7	17	1.27	45	3	21.27	-90.1
108		930	17.7	17	1.27	45	4	21.26	-90.1
109		960	17.7	11	1.27	0	1.5	24.42	-78.8
110		900	17.7	11	1.27	0	1.5	24.42	-78.8
111		960	17.7	11	1.27	0	2.5	24.42	-78.5
112		900	17.7	11	1.27	0	2.5	24.42	-78.5
113		960	17.7	11	1.27	0	3.5	24.41	-78.3
114		900	17.7	11	1.27	0	3.5	24.41	-78.3
115		960	17.7	11	1.27	0	4.5	24.43	-79.1
116		900	17.7	11	1.27	0	4.5	24.43	-79.1
117		960	17.7	11	1.27	-45	1.5	24.76	-81.2
118		960	17.7	11	1.27	-45	1.5	25.15	-81.1
119		960	17.7	11	1.27	-45	2.5	25.79	-81.2
120		900	17.7	11	1.27	-45	2.5	24.76	-81.2
121		900	17.7	11	1.27	-45	3.5	25.15	-81.1
122		900	17.7	11	1.27	-45	3.5	25.79	-81.2
123		960	17.7	11	1.27	45	1.5	21.29	-90
124		900	17.7	11	1.27	45	1.5	21.29	-90
125		960	17.7	11	1.27	45	2.5	21.29	-90
126		900	17.7	11	1.27	45	2.5	21.29	-90
127		960	17.7	11	1.27	45	3.5	21.28	-90
128		900	17.7	11	1.27	45	3.5	21.28	-90
129		960	17.7	6	1.27	0	1.5	24.42	-78.6
130		900	17.7	6	1.27	0	1.5	24.42	-78.6
131		960	17.7	6	1.27	0	2.5	24.42	-78.3
132		900	17.7	6	1.27	0	2.5	24.42	-78.3
133		960	17.7	6	1.27	0	3.5	24.41	-78.1
134		900	17.7	6	1.27	0	3.5	24.41	-78.1
135		960	17.7	6	1.27	0	4.5	24.43	-78.9
136		900	17.7	6	1.27	0	4.5	24.43	-78.9
137		930	17.7	6	1.27	-45	1.5	26.93	-81.3
138		930	17.7	6	1.27	-45	2.5	27.23	-81.2
139		930	17.7	6	1.27	-45	3.5	27.79	-81.2

140		930	17.7	6	1.27	45	1.5	20.71	-92.5
141		930	17.7	6	1.27	45	2.5	20.83	-92.7
142		930	17.7	6	1.27	45	3.5	21.04	-92.9
143		930	17.7	17	1.27	0	1.5	24.42	-78.8
144		930	17.7	17	1.27	0	2.5	24.42	-78.5
145		930	17.7	17	1.27	0	3.5	24.41	-78.2
146		930	17.7	17	1.27	0	4.5	24.43	-79.1
147		930	17.7	17	1.27	-45	1.5	23.64	-81.3
148		930	17.7	17	1.27	-45	2.5	24.08	-81.1
149		930	17.7	17	1.27	-45	3.5	23.73	-81
150		930	17.7	17	1.27	45	1.5	21.27	-90.1
151		930	17.7	17	1.27	45	2.5	21.27	-90.1
152		930	17.7	17	1.27	45	3.5	21.27	-90.1

Table 9- 5
A Tabulated Structure for Water Volumes for Sub basins and Basins

Subpolder Number	Overtopping Volume (V|OT)		Precipitation Rainfall Volume		Closures Water Volume		Breach Volume Elevation		Breach Volume Volume	
	Mean (ft^3)	StD (ft^3)	Mean (ft^3)	StD (ft^3)	Mean (ft^3)	StD (ft^3)	Mean (ft)	StD (ft)	Mean (ft^3)	StD (ft^3)
OW1	0.000E+00	0.000E+00	0.000E+00	0.000E+00	0.000E+00	0.000E+00	1.187E+00	5.937E-02	1.743E+08	4.571E+06
OW2	0.000E+00	0.000E+00	0.000E+00	0.000E+00	0.000E+00	0.000E+00	1.187E+00	5.937E-02	4.858E+08	9.056E+06
NOE1	0.000E+00	0.000E+00	1.655E+04	3.310E+03	4.724E+02	7.162E+01	1.187E+00	5.937E-02	4.461E+08	3.157E+07
NOE2	0.000E+00	0.000E+00	3.775E+06	7.551E+05	4.977E+02	9.954E+01	1.187E+00	5.937E-02	1.109E+09	1.355E+07
NOE3	0.000E+00	0.000E+00	2.703E+06	5.406E+05	0.000E+00	0.000E+00	1.187E+00	5.937E-02	3.059E+08	5.171E+06
NOE4	0.000E+00	0.000E+00	1.550E+01	3.100E+00	5.972E+02	1.194E+02	1.187E+00	5.937E-02	8.688E+07	2.631E+06
NOE5	0.000E+00	0.000E+00	9.367E+07	1.873E+07	0.000E+00	0.000E+00	1.187E+00	5.937E-02	2.463E+09	2.281E+07
OM1	0.000E+00	0.000E+00	0.000E+00	0.000E+00	0.000E+00	0.000E+00	1.187E+00	5.937E-02	7.075E+08	9.807E+06
OM2	0.000E+00	0.000E+00	0.000E+00	0.000E+00	0.000E+00	0.000E+00	1.187E+00	5.937E-02	6.399E+08	8.787E+06
OM3	0.000E+00	0.000E+00	0.000E+00	0.000E+00	0.000E+00	0.000E+00	1.187E+00	5.937E-02	2.480E+08	6.962E+06
OM4	0.000E+00	0.000E+00	0.000E+00	0.000E+00	0.000E+00	0.000E+00	1.187E+00	5.937E-02	7.016E+07	2.248E+06
OM5	0.000E+00	0.000E+00	0.000E+00	0.000E+00	0.000E+00	0.000E+00	1.187E+00	5.937E-02	4.371E+08	1.257E+07
SB1	0.000E+00	0.000E+00	0.000E+00	0.000E+00	0.000E+00	0.000E+00	1.187E+00	5.937E-02	1.753E+08	5.671E+06
SB2	0.000E+00	0.000E+00	0.000E+00	0.000E+00	0.000E+00	0.000E+00	1.187E+00	5.937E-02	1.367E+06	4.737E+04
SB3	0.000E+00	0.000E+00	0.000E+00	0.000E+00	0.000E+00	0.000E+00	1.187E+00	5.937E-02	1.491E+08	4.839E+06
SB4	0.000E+00	0.000E+00	0.000E+00	0.000E+00	0.000E+00	0.000E+00	1.187E+00	5.937E-02	1.581E+07	2.990E+06

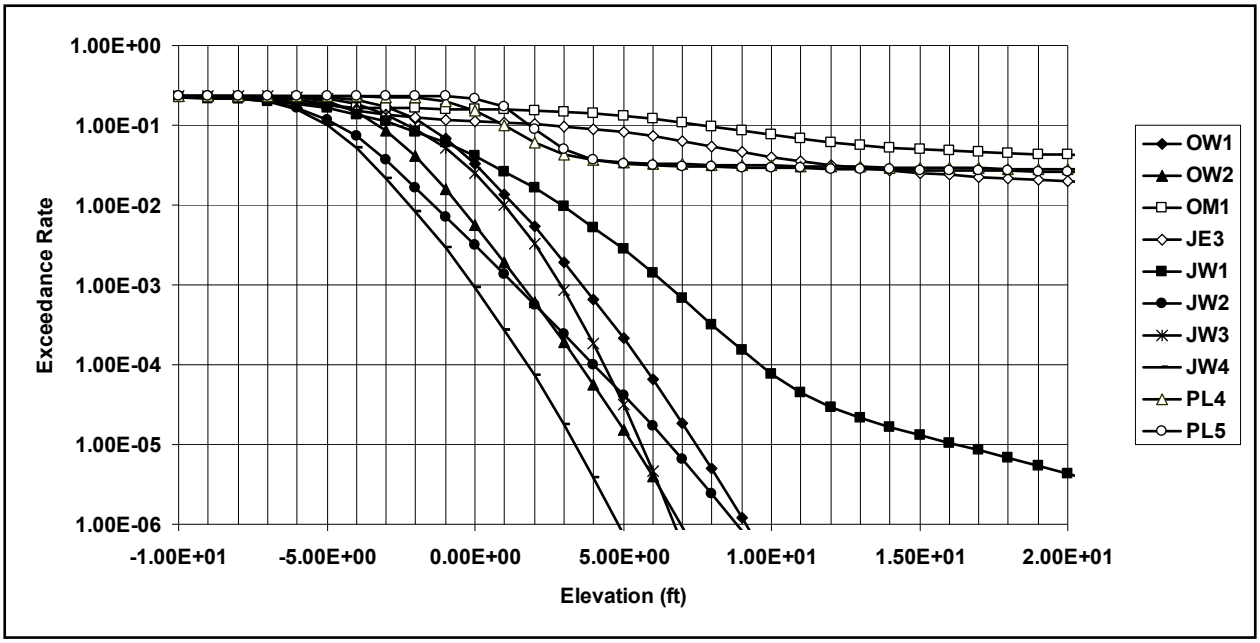

Figure 9-11 Example Elevation-Exceedance Curve

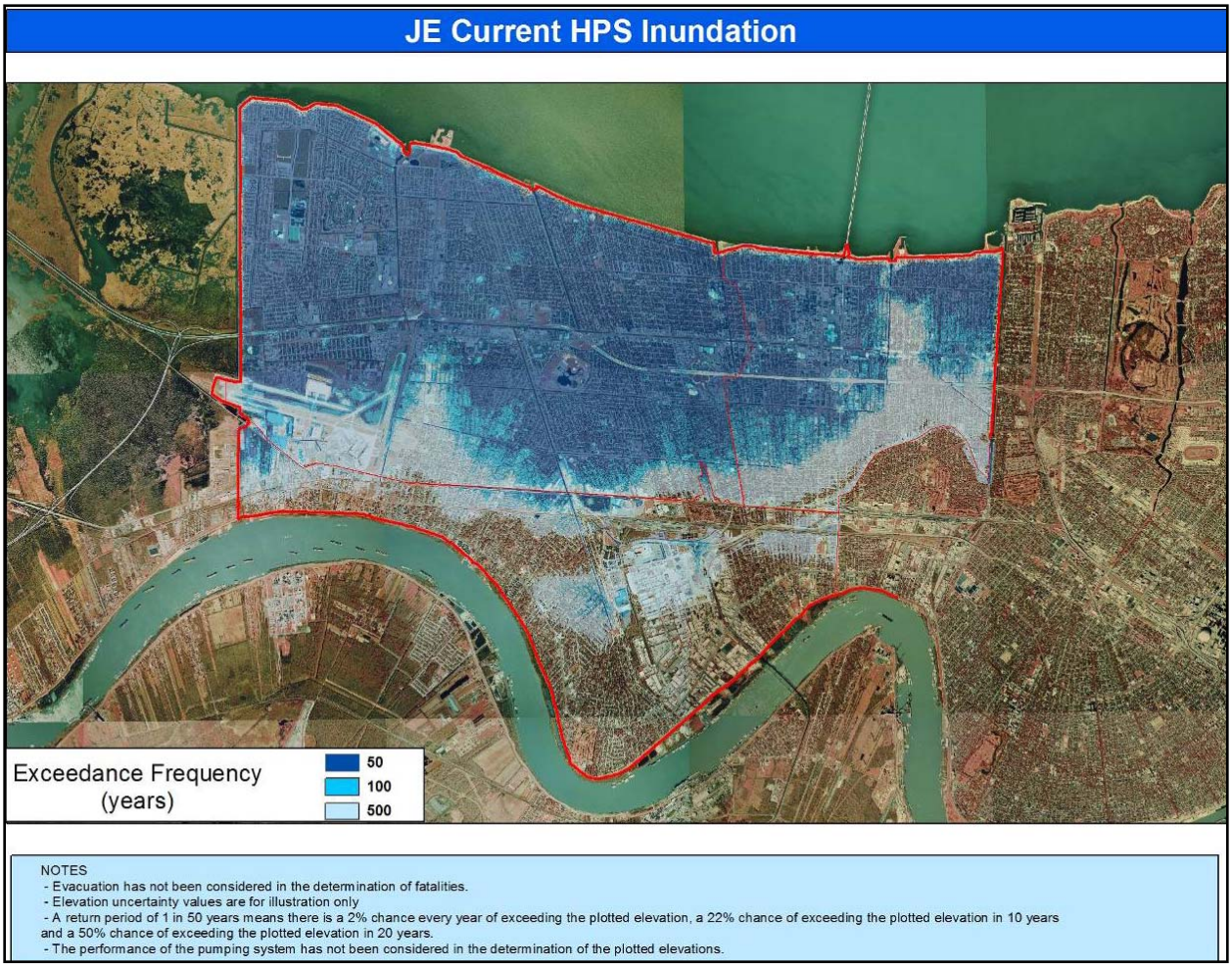

Figure 9-12. Sample Inundation Map

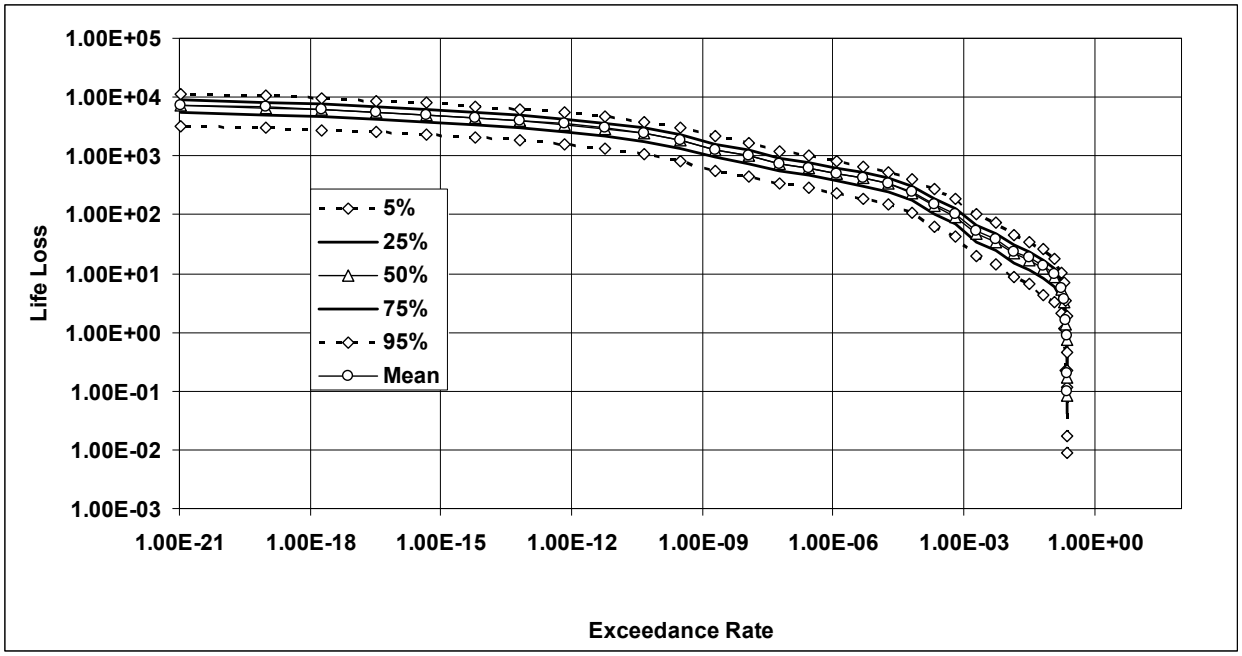

Figure 9-13 Example Life Loss –Exceedance Curve

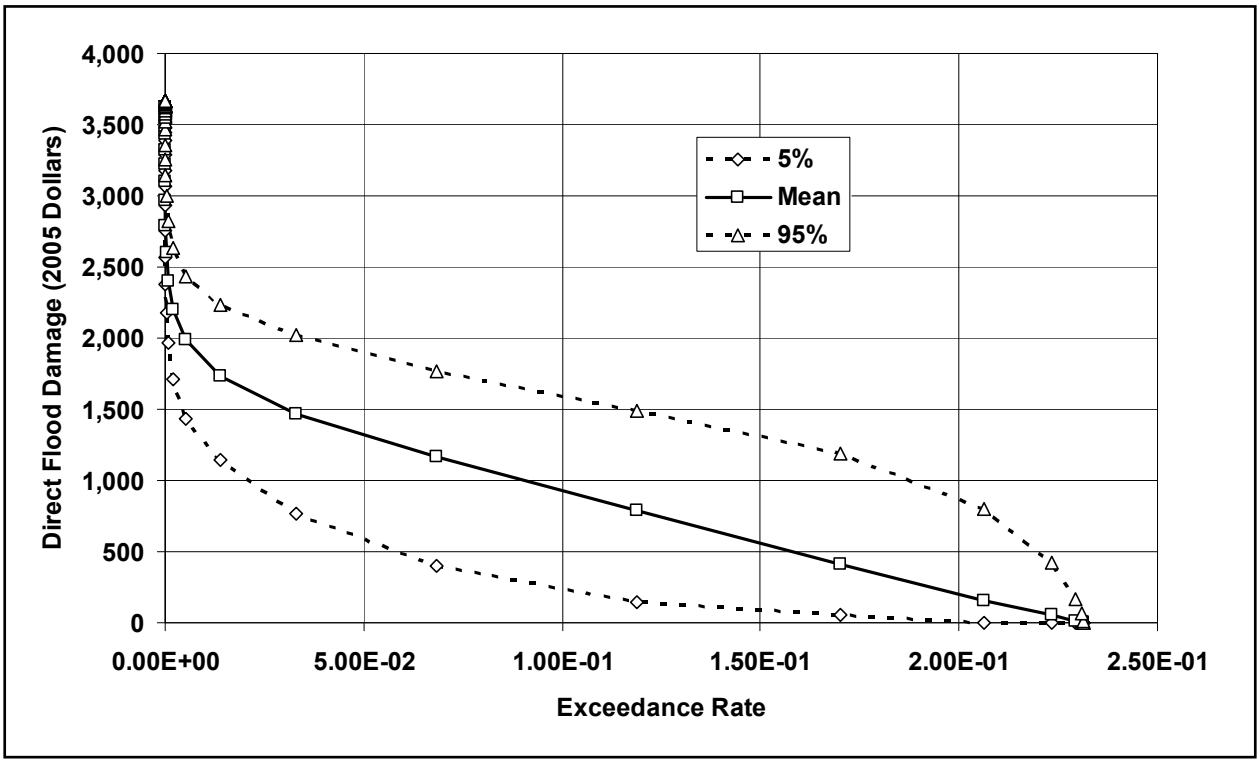

Figure 9-14. Example Damage-Exceedance Curve. Note: Direct Flood Damages (Millions of 2005 Dollars)